01563

MISCELLANEOUS PAPER NO. 2-777

HYDRAULIC DESIGN OF ROCK RIPRAP

by

F. B. Campbell

February 1966

Sponsored by

Office, Chief of Engineers
U. S. Army

Conducted by

U. S. Army Engineer Waterways Experiment Station
CORPS OF ENGINEERS
Vicksburg, Mississippi

01563

MISCELLANEOUS PAPER NO. 2-777

HYDRAULIC DESIGN OF ROCK RIPRAP

by

F. B. Campbell

February 1966

Sponsored by

Office, Chief of Engineers
U. S. Army

Conducted by

U. S. Army Engineer Waterways Experiment Station
CORPS OF ENGINEERS
Vicksburg, Mississippi

MISCELLANEOUS PAPER NO. 2-777

HYDRAULIC DESIGN OF ROCK RIPRAP

by

F. B. Campbell

February 1966

Sponsored by

Office, Chief of Engineers
U. S. Army

Conducted by

U. S. Army Engineer Waterways Experiment Station
CORPS OF ENGINEERS
Vicksburg, Mississippi

ARMY-MRC VICKSBURG, MISS.

FOREWORD

The decision to prepare this paper was reached during a conference at the U. S. Army Engineer Waterways Experiment Station (WES) on 16 March 1965 attended by Mr. S. B. Powell, representing the Office, Chief of Engineers (OCE), and staff members of the WES Hydraulics Division. The conference was conceived through the encouragement of Mr. J. H. Douma, OCE. The aspects of a rational approach to the hydraulic design of rock riprap were discussed.

This paper was prepared by Mr. F. B. Campbell, Chief, WES Hydraulic Analysis Branch, with the technical assistance of the Analysis Section staff under the supervision of Mr. R. G. Cox. The treatment of the stability of riprap on a streambank as well as other analyses was prepared by Mr. M. Dorl. The analysis of the field observations of velocity distribution for the Feather River Site 12, furnished by the Sacramento District, was performed by Pfc. J. S. Watkins. The graph on "Stable Rock Size" was based on an earlier study by Mr. Cox in connection with the preparation of Hydraulic Design Criteria Chart 712-1. Numerous aspects of the design problems treated are the outgrowth of stimulating discussions with Mr. S. B. Powell who also furnished numerous reports on field investigations of riprap which were not available in the WES Research Center Library.

This presentation was prepared under the general supervision of and with the sympathetic interest of Mr. E. P. Fortson, Jr., Chief, Hydraulics Division, and Mr. J. B. Tiffany, Technical Director. Col. John R. Oswalt, Jr., CE, was Director, WES, during the preparation and publication of this paper.

CONTENTS

	Page
FOREWORD	iii
GLOSSARY	vii
SUMMARY	ix
PART I: INTRODUCTION	1
Purpose	1
Scope of This Paper	1
The Design Problem	2
PART II: UNIFORM TRANQUIL FLOW WITH FULLY DEVELOPED TURBULENCE	3
Straight Channels	3
Channel Bends	12
Field Data Needed for Design	16
PART III: HIGHLY TURBULENT FLOW	18
Bottom Riprap	18
Bank Riprap	19
PART IV: CONCLUSIONS	22
LITERATURE CITED	23
PLATES 1-12	
APPENDIX A: STABILITY OF CUBICAL RIPRAP ELEMENTS OF BANK SLOPES	A1
APPENDIX B: RIPRAP INVESTIGATIONS NEEDED	B1

GLOSSARY

A_f Frontal area of cube

C_D Drag coefficient

C_s Stability coefficient $= (n^2 + 1)^{-1/2} F_p^{-2} = \frac{1}{7.41} \tan \phi \, (\sin \phi + \cos \phi)$

d Depth of flow

d_1 Flow depth entering stilling basin

d_2 Theoretical downstream depth for hydraulic jump

D Drag force $= C_D \gamma_f A_f \frac{V_K^2}{2g}$; also, stone diameter

E_2 Isbash stability coefficient

F_p Particle Froude number $= \frac{V_K}{\sqrt{g\ell}}$

F_1 Froude number entering stilling basin

g Acceleration due to gravity

H_s Observed wave height from crest to trough

K Equivalent stone diameter

K_s Nikuradse's sand grain diameter

ℓ Length of side of cube

M Factor $= [1 + \sin (2\phi)]^{3/2}$

n Cotangent of slope angle

Q Discharge

r Bend radius

R Hydraulic radius

s Water-surface slope

T Overturning force; also thickness of riprap blanket

V Velocity of a flow profile at a distance from the boundary

V_* Shear velocity of flow at a boundary

V_K Velocity of fluid at height $\ell/2$ above cube top; also velocity of f[illegible] near a boundary (equation 2)

w Channel width at water surface

W Weight of cube on side slope under fluid

W_n Weight normal to side slope

W_o Weight of cube on bottom under fluid

W_t Weight tangential to side slope

y Distance from flow boundary

Y Distance from center line of stone riprap perpendicular to boundary

Y_f Distance from top of riprap perpendicular to boundary

γ_f Specific weight of fluid

γ_p Specific weight of particle in air

γ_s Submerged specific weight of particle = $\gamma_p - \gamma_f$

θ Channel bend deflection angle; also angle of resultant force acting [illegible] stone on bank slope

ρ Fluid density

τ_a Average wall shear in a straight approach

τ_b Highest wall shear caused by a bend

τ_o Wall shear

SUMMARY

This paper summarizes a study of open channel flow conditions affecting riprap design and suggests a design procedure based on hydraulic principles rather than on rule-of-thumb formulas. Riprap design is idealized by study of the stability of a cubical element. Field and laboratory investigations required for the development of firm design criteria are recommended.

HYDRAULIC DESIGN OF ROCK RIPRAP

PART I: INTRODUCTION

Purpose

1. The serious need for valid criteria for the hydraulic design of riprap has been apparent for some time and the Waterways Experiment Station (WES) has been working on various phases of the problem for the past eight years at the request of the Office, Chief of Engineers (OCE). This report illustrates the application of the results to date of the WES investigations into pertinent theory, experimental work, and field experience to the problem of designing riprap for various channel conditions. Much more laboratory work and field observations are needed before firm criteria can be established. However, it is believed that sufficient information is available from scattered sources, and modern fluid mechanics concepts have advanced to a point where tentative design criteria can be outlined.

2. Optimum use of current knowledge should result in lower construction costs and should reduce maintenance costs necessary to replace riprap damaged and removed by floods. However, no single specification for riprap can be employed to cover all cases. Furthermore, hydraulic engineers should gain an understanding of modern fluid mechanics principles involved and seek laboratory and field information appropriate to the specific situation for which riprap is to be designed.

Scope of This Paper

3. The treatment of the design of riprap presented in this report will follow the outline given below. It begins with the simplest problem with the least number of independent variables and progresses through a sequence of problems of increasing complexity.

- a. Uniform tranquil flow with fully developed turbulence
  - (1) Straight channels
    - (a) Bottom riprap, no appreciable lateral slope

(b) Bank riprap, appreciable side slope

(2) Channel bends

b. Highly turbulent flow (Example: Immediately downstream from energy dissipators)

(1) Bottom riprap (Example: Downstream from stilling basin end sills)

(2) Bank riprap

(a) Wave action effect

(b) Side roller or bank eddy effect

The Design Problem

4. The designer needs to determine the effective size of riprap which will be stable for the velocity acting on the rock. In order to determine this velocity, he must estimate the velocity profile normal to the bottom. For this purpose, field measurements of velocity distribution over riprap of known size and gradation are needed. In addition, the problems of effective size of graded riprap which will establish the roughness dimension, and the effective size for stability considerations require further study in the laboratory and the field. However, considerable experimental information has been collected for the preparation of Hydraulic Design Criteria Chart 712-1.[1*] The shape of the rock, whether rounded as with cobbles or angular as with rock blasted from a quarry, and the method of placement are factors which contribute to the stability.

* Raised numerals refer to similarly numbered items in Literature Cited at end of text.

5. In the development of a design procedure, the level bottom of a channel will be considered first. The increased weight of stone needed for stability on the channel bank and in bends will then be related to bottom riprap in a straight channel.

Straight Channels

Bottom riprap

6. The following analysis does not apply to nonuniform flow where there is rapid acceleration or deceleration of flow. It is applicable to natural stream channels where the width is normally more than five times the depth.

7. Velocity profile. The first step in the analysis is to estimate the velocity profile which will exist at a given normal to the boundary during the design flood. This problem is tractable by use of modern concepts of fluid mechanics. In his classical paper on "Law of Turbulent Flow in Open Channels," Keulegan[2] used Nikuradse's research on pipe roughened with uniform sand grains and developed the following equation:*

$$\frac{V}{V_*} = 8.5 + 5.75 \log \left(\frac{y}{K_s} \right) \quad (1)$$

where V is the velocity of a profile at distance y from the boundary, V_* is the shear velocity at the boundary, and K_s is Nikuradse's sand grain diameter. It should be emphasized that nondimensional equation 1 applies equally well to the profile region near the boundary of an open channel as to the boundary region near the wall of a circular pipe. Some authorities call this relation the inner law and the relation for the flow near the center of the pipe the outer law. This treatment is concerned only with the inner law.

8. More recently, Rouse[3]** has published another dimensionless

---

* See equation 23, page 732, in reference 2.
** See equation 102, page 103, in reference 3.

equation which is also based on research by Nikuradse. The Rouse equation is:

$$\frac{V}{V_K} = 0.68 \log \left(\frac{y}{K_s} \right) + 1 \tag{2}$$

where V_K is a velocity near the boundary and K_s is the same as in equation 1. It should be noted that if equation 1 is divided by 8.5 and the velocity ratios equated, then:

$$\frac{V}{V_*} = 8.5 \frac{V}{V_K} \tag{3}$$

Eliminating the variable V , the following relation results:

$$V_K = 8.5 \, V_* \tag{4}$$

In this paper, V_K will be considered to be the velocity acting on an isolated piece of rock.

9. Dimensionless velocity profile. Rouse's curve[3] for a rough boundary velocity profile has been adapted for this treatment as indicated in plate 1. The velocity profile in plate 1 is a plot of equation 2. It should be noted that when $y/K_s = 1.0$, the term $0.68 \log (y/K) = 0$, and V/V_K must then be 1.0. This is a convenient device for interpreting laboratory and field observations. In this paper, V_K is assumed to have a $y = K_s$.

10. Field measurements. There is a scarcity of both laboratory and field measurements of the velocity profile for a known roughness value. Extensive field tests on an artificial channel with known riprap size below Dorena Dam were reported in 1952.[4] The main test reach was 160 ft long, the bottom fairly steep, and the flow nonuniform. Average velocities increased from 4.5 fps to 11.4 fps in this reach. However, velocity measurements were inadequate to develop good velocity profiles.

11. Field measurements on Feather River.* The U. S. Army Engineer

---

* Unpublished data on riprap investigations furnished by the District Engineer, U. S. Army Engineer District, Sacramento, in 1960.

District, Sacramento, measured velocity profiles at a number of sites on the Feather River where riprap of known gradation had been placed. Although most of the sites were affected by bends in the river, site 12 was located on a straight reach and measurements at that site were selected for further study. A cross-sectional plot of the velocity distribution at site 12 is shown in plate 2. In a preliminary examination, isovels were carefully sketched. These showed isolated peaks of high velocity which could have been the result of a mound of riprap upstream or some other such local disturbance. The isovels in plate 2 have been normalized, and the Y_f values scaled for corresponding isovels at the four sections drawn perpendicular to the boundary. The velocity profiles at these sections are plotted in a dimensional semilogarithmic graph (plate 3). A single straight line can be drawn through the points which closely approximates the velocity profile of the four sections.

12. Effective roughness. Several assumptions as to the stone diameter representing the effective roughness K were made for study on a dimensionless semilogarithmic graph. Information from the Sacramento District indicated that the average riprap stone diameter at site 12 on the Feather River was approximately 4.6 in., or 0.38 ft. The coordinate of $Y = K$ on the dimensional graph (plate 4) with a depth correction of 0.19 ft, or half the K dimension, indicated a value V_K of 2.46 fps. Dimensionless graphs for 4.6-, 5-, and 6-in.-diameter stones were drawn using the corresponding values of K and V_K. All of the curves were very close together, and the average stone diameter of 4.6 in. was adopted as representing the proper dimensionless profile.

13. The general equation for the dimensionless profile is:

$$\frac{V}{V_K} = A \log\left(\frac{y}{K}\right) + B$$

As noted in paragraph 7, Keulegan's constants for A and B using shear velocity are 5.75 and 8.5, respectively, whereas Rouse's constants using V_K instead of V_* are 0.68 and 1.0. If the K for Feather River site 12 is 0.38 ft, the V_K is 2.46 fps (plate 4). From the corresponding dimensionless profile, the slope of the line of best fit gives constant A as 0.95. Although it departs considerably from the value $A = 0.68$ based on Nikuradse's uniform sand grain, similar departures for velocity distribution were found in comparing dimensionless plots in large flood-control tunnels.[5] These departures are believed to be the result of a mixed roughness size as contrasted to the uniform grain size of Nikuradse.

14. Effect of depth. The Feather River site 12 tests were made at a low stage on the river and cannot be expected to apply to the design stage. The shear velocity for an open channel can be written:

$$V_* = (Rsg)^{0.5} \tag{5}$$

where R is the hydraulic radius, s is the surface slope, and g the gravitational constant. If it is assumed that the general slope of the stream at the low stage of measurement is the same as the slope for the design flow, the following ratio can be written for shear velocity:

$$\frac{V_{*L}}{V_{*H}} = \left(\frac{d_L}{d_H}\right)^{0.5} \tag{6}$$

where subscripts L and H refer to low and high stages and d is the depth of flow along the velocity profile normal to the boundary. Furthermore, since V_K is proportional to V_*, the following ratio can be written:

$$\frac{V_{KL}}{V_{KH}} = \left(\frac{d_L}{d_H}\right)^{0.5} \tag{7}$$

An estimation of depth for design flow is not simple if the bottom is an alluvium which scours deeply during floods. Measurements from existing bridges or cableways can sometimes give an indication of depth of scour upon which to base an estimate. Obviously, the manner in which the bank riprap restrains erosion at its toe can influence the local wall shear if bottom scour is deep. In any case, the depths should be measured normal to the boundary in the analysis of the field data. Velocity profiles measured too close to the water's edge have no practical significance in attempting to relate shear or bottom velocity at low stages to these quantities at a higher design stage. Certain stream dynamics aspects of the problem have been analyzed recently by Lundgren and Jonsson.[6]

15. Effect of surface slope. Equation 5 for shear velocity indicates that the longitudinal water-surface slope s is an independent variable equally as important as depth d in determining the design velocity. In order to account for the effect of longitudinal slope of the water surface on the design velocity V_K, the following ratios are applicable:

$$\frac{V_{KH}}{V_{KL}} = \left(\frac{d_H s_H}{d_L s_L}\right)^{0.5} \qquad (8)$$

If velocity profiles and depths are measured at too low a stage, the stream surface slope will probably be substantially different from that which is to be expected at design stage. Streams in nature at low stage are usually characterized by a series of pools and controls. The slope will be less than at flood stage in the pools and greater than at flood stage over the controls. It is therefore important to set slope stakes and measure the slope at the time the vertical velocity distribution and depths are measured. Finally, the hydraulic engineer must have sufficient information to estimate the slope and depth at design stage.

16. Effect of riprap size gradation. On any one river, the field measurements of velocities, depths, and water-surface slopes should be made at sites where riprap has been recently placed. The most economical riprap available for the locality is commonly used, even though it may not have an ideal gradation. Sufficient information is not available to determine the ideal gradation, and with the present state of the art there is no basis for making an economic study involving first cost and costs of maintenance and repair. However, certain basic facts should be recognized in regard to gradation. If the span of the stone sizes is very great, say from the size that 10 percent of the stone is smaller to the size that 90 percent of the stone is smaller, it may be characterized as a broad size span. At the other extreme is the narrow size span in which there is little difference between the size of the 10 percent smaller and 90 percent smaller stones. From the hydraulic design standpoint, a nearly uniform

rock size, or narrow size span, is ideal, but would hardly be realized except in the locality of large talus deposits at the foot of rock cliffs or palisades where the large rock is at the toe and the small rock at the top of the slope.

17. It is understood that some Corps of Engineers Districts permit the use of a broad size span as follows:

$$D_{100} \leq 5D_{50}$$

where D_{100} is that size of which 100 percent of the stone is smaller. Such a specification further states in regard to fines that:

$$D_{15} \geq 0.25D_{50}$$

In other Districts, the smaller size span is specified as follows:

$$D_{100} \geq 3 \text{ or } 4D_{50}$$

These differences probably indicate the most economical riprap available at specific localities. The riprap with the smaller size span would no doubt be more stable because there are fewer small stones to be lost during flood stage. Experiments with the effect of gradation can best be accomplished in the laboratory because synthetic gradation is less costly on a small scale.

18. Effect of riprap thickness. The thickness of the riprap blanket and the gradation are interrelated. With a broad size span, isolated pieces of large rock will protrude into the flow. The flow will accelerate around the large stone and remove the smaller particles. This phenomenon is similar to the deep scour alongside and just downstream from bridge piers. As a general guide, under the present state of the art, the thickness of the blanket T should be

$$T = 1.5D_{max}$$

where D_{max} is the size of which 100 percent of the stone is smaller.

19. Stable rock size. To estimate the required size of rock which is stable for a given velocity, the 50 percent size is used. The Airy law[7,8,9] states that the weight required for stability varies as the sixth power of the velocity acting on the rock. In the Transactions of the Second Congress on Large Dams, published by the Government Printing Office in 1936, S. V. Isbash[10] presented experimental coefficients to be used with Airy's law. Other experimental information used for Hydraulic Design Criteria Chart 712-1 (paragraph 4) confirms the Isbash recommendations in general. A coefficient $E_2 = 1.20$ is used as the basis of the Isbash curve in plate 5. Because cobbles are used for riprap in some localities, an arbitrary curve to the left of the Isbash curve is presented for use with cobbles. Another to the right of the Isbash curve is marked for use with quarry rock. In general, cobbles approach a spherical shape and rock blasted from a quarry approaches a cubical shape. More experimental information is needed for quarry rock and cobbles.

20. The method of placement of the riprap can be expected to affect the stability. Random dumping of riprap is the most common placement method. Hand-placed riprap, as placed by the New England Division using WPA funds, has been shown to be very stable during floods. Tamping riprap with a heavy steel plate, as in a few instances in the Portland District, can be expected to wedge the rock tightly into place. The curves in plate 5 are considered applicable only to random-dumped riprap.

Bank riprap

21. The preceding considerations are applicable to the bottom of a straight channel. Certain analytical procedures can be used to relate stable stone size on the bottom to the corresponding size on a bank or lateral slope. The analysis can be made with an idealized shape such as a sphere (representing well-worn cobbles) or cube (representing rock blasted from a quarry). As most riprap is probably quarry rock, the isolated cube was selected for analysis. Definition sketches are shown in plate 6 and the complete analytical treatment is included as Appendix A.

22. Plate 6a indicates a cube having weight W_o resting on the bottom and a larger cube with weight W resting on the bank. The objective of the design problem is to estimate the ratio of the weights W/W_o

for any given weight W_o, velocity V_K, and side slope n. Plate 6b indicates that the cube on the slope has a component normal to the slope W_n and one down the slope W_t. Plate 6c shows that the gravity component W_t and the drag component D combine to form a resultant T at a specific angle ϕ to the direction of flow. These general concepts were noted by Lane and Carlson.[11] The analysis in Appendix A assumes that the cube is dislodged by rotating over a hinge line normal to the resultant force causing the instability.

23. The analysis in Appendix A indicates that the stability of a cube on a slope is a function of the Froude number F_p of the particle size:

$$F_p = \frac{V_K}{(g\ell)^{0.5}} \tag{9}$$

where V_K is the velocity acting on the stone and ℓ is the length of a side of the cube. The stability is also a function of the side slope n. These two functions can be combined into a stability coefficient C_s as follows:

$$C_s = \frac{1}{F_p^2\,(n^2 + 1)^{0.5}} \tag{10}$$

Plate 7 shows the relation between C_s and a factor M in the final equation yielding the following ratio of weights.

$$\frac{W}{W_o} = M\left(\frac{n^2 + 1}{n^2 - 1}\right)^{3/2} \tag{11}$$

24. In the analysis, it is necessary to assume a drag coefficient. For this purpose, the curve for quarry rock in plate 5 is used. This is not a pure drag coefficient but includes any vertically upward or downward force on the cube. The result is a coefficient which combines drag and lift.

25. From equations 10 and 11, it can be seen that there are two separate functions of the side slope n. The following tabulation pertaining to side slope functions is included for the convenience of the designer.

Slope, n	$(n^2 + 1)^{0.5}$	$\left(\frac{n^2 + 1}{n^2 - 1}\right)^{3/2}$
2	2.24	2.15
3	3.16	1.40
4	4.12	1.21
5	5.10	1.125
6	6.08	1.085

This tabulation together with plate 7 can be used to determine the weight ratio W/W_o .

Toe protection

26. One of the most troublesome problems pertaining to riprap blankets on streambanks is the design, construction, and maintenance of the toe. The highest boundary shear on the bank is near the bottom and is approximately equal to that acting on the adjacent bed (plate 8a). If the bed is an alluvium (sand and fine gravel), it is natural for the toe of the blanket to be undercut during high water. There are two design concepts of toe protection extant in the Corps of Engineers, each with its own advantages and disadvantages. These schemes are designated the "toe trench" and the "thickened toe" in this paper and are shown in plate 8. This plate does not show dimensions or slopes, as each design must be assigned its own dimensions dependent upon the local anticipated bed scour and the character of the riprap available. More field information is needed on the behavior of these designs during flood passage.

27. Toe trench. The toe trench shown in plate 8b involves excavation and preplacement of rock below the low-water bed of alluvium. It has the advantages of positive knowledge of the location of the toe protection stone, and a side slope stability designed to withstand the high boundary shear estimated for flood stage.

28. A disadvantage of the toe trench is the requirement for underwater excavation of the trench in alluvium. Another disadvantage is that the angle of repose of the toe trench itself may be fairly flat so that a large quantity of rock may eventually be required to fill the trench. Also, in the case of a narrow stream, the toe trench type of construction further narrows the cross section at flood stage. If appreciable narrowing

results, the longitudinal water-surface slope would be increased, causing increased bed shear and deeper scour.

29. Thickened toe. The thickened toe (plate 8c) design anticipates the scour line of the alluvial bed and purposely provides for a steeper slope near the toe so that the rock can roll down over the eroded bed beyond. Its principal advantage is the elimination of an underwater trench, but it does assume that the bank on the steeper back slope will be temporarily stable until the rock is placed. The thickened toe type of design would result in a minimum constriction of the stream cross section during flood and reduce the excessive scour caused by such constriction.

30. The disadvantage of the thickened toe design is that the smaller size rock would probably wash outward into the stream and their function as a void filler would be lost. Also, it is difficult to estimate the percentage of large size rock needed; however, it seems desirable that the size span of the gradation should be narrow. Furthermore, opportunities for observation of the field performance of the thickened toe during floods are limited. Postflood inspection would require subaqueous hand excavation, possibly by jetting.

31. Complete field information on this aspect of the riprap problem should be obtained as indicated in paragraphs 2 and 4. In addition, soil mechanics engineers should be consulted in estimating the stable saturated slope of both the in situ alluvium and the bank material. Most natural stream channel riprap is involved with bends or curved reaches which are discussed subsequently.

Channel Bends

Bend problems

32. In natural stream channel stabilization, riprap is most commonly used in the vicinity of bends. The foregoing discussion of straight channels considered first the problem of the channel bottom which was treated essentially as a simple two-dimensional problem involving the velocity profile and the roughness as related to the distance from the bottom. The effects of total depth and longitudinal water-surface slope were also discussed.

The stability of riprap on the bank of a straight channel introduced the lateral dimension of bank slope. One of the gravity components of bank-slope riprap resists movement, while the other must be coupled with a drag-type force tending to displace the rocks. In addition to the considerations pertaining to a straight channel, the banks of a channel bend involve other variables, the effects of which have not been fully explored.

33. One of the simpler geometrical approaches to the bend problem is to assume a uniform, trapezoidal cross section. The geometry of the bend can then be defined in the following terms:

$$n \ , \ \frac{r}{w} \ , \ \theta \ , \ \text{and} \ \ \frac{w}{d}$$

where n is the ratio of the horizontal to the vertical dimensions of the side slope, r is the radius to the center line of the channel, w is the channel width at the water surface, θ is the central angle, and d is the depth of flow. Laboratory experiments conducted on bends of trapezoidal channels at the Massachusetts Institute of Technology (MIT),[12] the Bureau of Reclamation (USBR),[13] and the University of Iowa[14] are discussed below.

Laboratory experiments

34. Tests. Tests were conducted on smooth channel bends at MIT, USBR, and Iowa. In addition, MIT made limited tests on rough channel bends. In the latter tests, the channel was roughened by fixing 0.18- by 0.10- by 0.10-in. parallelepipeds to the boundary in a random manner, resulting in a roughness height of 0.10 in. In all tests, Preston tubes[15] were used to measure boundary shear directly. A comparison of test conditions and results is given in the following tabulation.

Laboratory	Type Channel	Side Slope	Invert Width, in.	r/w	θ, deg	w/d
MIT	Smooth	2:1	12	3.45	60	10.0
				2.94		8.0
				2.50		7.0
			24	1.67		12.0
				1.37		8.8
				1.25		8.0

(Continued)

Laboratory	Type Channel	Side Slope	Invert Width, in.	r/w	θ, deg	w/d
USBR	Smooth	1-1/2:1	24	3.76	15	5.7
Iowa	Smooth	1:1	72	4.18	90	19.0
				4.00		14.0
				3.99		13.7
				3.99		13.7
				3.73		10.0
MIT	Rough	2:1	24	1.49	60	10.0
				1.25		8.0

The plan of the 24-in.-wide MIT test channel is shown in plate 9. Those of the USBR and Iowa channels are given in plate 10. The principal difference in the geometry of the MIT 12-in. and 24-in. channels was the invert width.

35. Results. The lines of equal boundary shear are presented in plates 9 and 10 in terms of the ratio of wall shear τ_o at the point to the average wall shear τ_a in the straight approach. It can be noted that the highest wall shear τ_b caused by the bend occurs downstream from the outside of the bend in the USBR and MIT tests. Another area of high wall shear is located at the inside of the bend. In the Iowa tests, only the shear within the bend was measured. For purposes of correlating the results, the maximum wall shear has been related to the average approach wall shear as τ_b/τ_a and plotted against the respective ratios of r/w (plate 11). The equation of the graph is for the line of best fit using the smooth channel data points. Even with a limited range of values of r/w, there appears to be a power law relating these values to τ_b/τ_a. Although only two measurements are available for rough channels, the results plotted in plate 11 indicate the same slope of curve as for the smooth channel data. The shear velocity is commonly expressed in terms of wall shear as follows:

$$V_* = (\tau_o/\rho)^{0.5} \tag{12}$$

where ρ is the fluid density and is assumed here to have a value of 1.94 slugs per cu ft. Considering the proportionality expressed in equation 4, the ratio of effective velocities acting on the rock can be written:

$$\frac{V_{Kb}}{V_{Ka}} = \left(\frac{\tau_b}{\tau_a}\right) \tag{13}$$

This equation is valid only for a case where the V_{Ka} in the straight approach is based upon an average wall shear for the section.

Applicability of experimental results

36. An examination of the research results on wall shear distribution in a channel bend indicates that further extensive investigation needs to be accomplished. Laboratory studies have been concerned mostly with smooth walls because the use of a Preston tube has been considered appropriate in the past for only such boundaries. However, a modified Preston tube was used successfully in the MIT rough channel tests. The actual pattern of wall shear distribution appears to be similar for both smooth and rough boundaries (plates 9, 10, and 11). However, available data indicate higher shear ratios for rough boundaries. Lacking the proper experimental simulation of riprap, one can use the existing results as a guide to judgment. Of greatest practical importance is the fact that a uniform, trapezoidal cross section around the bend deviates grossly from the geometry formed in a natural stream with an erosive alluvial bed. It has long been recognized that a natural streambed will develop a bar on the inside of the bend and a deep scour hole on the outside. Extreme examples of this phenomenon are experienced on the Lower Mississippi River where scour holes may reach a depth of 200 ft. However, for streams of less total shear velocity and bed alluvium more resistant to erosion, no such extreme scour hole depths should be expected. It may be that a laboratory channel of triangular cross section with a short, steep bank at the outside of the bend and a long, flat leg at the inside would approximate the natural condition. Field measurements of cross sections are needed as a guide. Pending further laboratory studies, the designer should consider the effective radius to the mean curvature of the thalweg of a natural stream. It appears reasonable to use a smaller value of top width than that measured in nature in using plate 11.

Recommended current design practice

37. It is apparent from the considerations discussed above that any comprehensive laboratory study will be costly and time consuming. In the meantime plates 9 and 10 can be used as guides to the general location of high wall shear on the outside of the bend, and plate 11 can be used to supplement judgment as to the relation of maximum shear values in the tangents to those of the bends.

Field Data Needed for Design

38. The most pressing current need is for field measurements of depths and velocities at selected locations where new riprap of known gradation and shape has been placed. Observations on both straight and curved reaches are needed. In view of the heterogeneity of the independent variables of the problem as found in the field, multiple cross sections should be observed. Analyses similar to that described previously for Feather River site 12 should be made.

39. The vertical velocity profiles should comprise at least seven velocity observations in a single vertical with special attention given to the bottom half of the depth. A larger range in variation of the quantities measured can be expected in the bends than in the tangent reaches. It is therefore important to have a larger number of observations in the bends selected for observation. The objectives of the velocity measurements are twofold: (a) to obtain average values, and (b) to obtain extreme values. Average values are of interest in establishing the constants for the general laws of riprap behavior, and extreme values are of interest in conservative design. The turbulent nature of natural streamflow will cause both short-period and long-period variations in the velocity at a given point. To obtain a reliable average velocity at a point, the current meter revolutions should be recorded for from 1 to 1-1/2 min.

40. As mentioned previously, synthetic size gradation in the field is a costly procedure. However, there is a wide range of size spans and shapes in the most economical, available riprap used by the various CE Districts. Reasonably accurate measurements of size gradations and

photographs of typical rock shape are an important part of the record. A comparative study of the field data from various localities (both the effective roughness size for a given average velocity profile and the effective size for stability) could yield much information of value to future design. Field results have a dual role in guiding future laboratory studies and in affording information for immediate use in current design.

41. Final check on the effective rock size on riprap test sections requires a record of the sizes of stone which have been displaced during floods. Samples of in-place stones of three size groups larger than the estimated average stone in test installations should be painted with different colors. These stones should be numbered and their locations recorded so that the size of rock displaced by a subsequent flood can be determined. Photographs of the observation stones should be made. Precision in estimating the stone size and weight is neither practical nor necessary in view of the present state of the art. Postflood examination need not determine how far the observation stone has been transported, but only what size groups have been dislodged.

PART III: HIGHLY TURBULENT FLOW

42. The preceding discussion is applicable only to the normal turbulence found in natural stream channels. A special situation exists downstream from energy dissipators, at a severe restriction of a stream channel which causes a large head drop, and at other places where man-made structures cause highly turbulent flow. As indicated in paragraph 3b, two problems exist: one involves the bottom riprap, and the other the bank riprap. Different hydraulic and stability phenomena are encountered in the separate areas. The problems are so complex in highly turbulent flow that little or no analytical approach exists at present. Model studies are thus required for solution of the riprap problem in highly turbulent areas. Flow just downstream from a stilling basin is used as an example of design of riprap for highly turbulent flow by means of model studies.

Bottom Riprap

43. A terminal structure for a spillway or outlet works may be a flip bucket, roller bucket, or stilling basin. The stilling basin involves numerous independent geometric variables such as lateral spread of the entering flow; the size, shape, lateral spacing, and longitudinal location of baffle piers; and the heights, shape, and longitudinal location of the end sill. The bottom upon which riprap is placed beyond the basin may be level or sloped upward or downward. In addition to the innumerable combinations of geometric variables are the hydraulic variables of Froude number of the entering flow and tailwater depth. Not only do the many combinations of these independent variables have an unpredictable effect upon the bottom velocity, but the issuing flow does not have a turbulent boundary layer which can be predicted. In addition to these variables, the large turbulence pulses create unknown vertical pulses on the bottom riprap. It is therefore obvious that hydraulic model studies offer the best means for determining the stable size of bottom riprap.

44. In the cases of outlets from culverts or other small structures where model studies are not justified, the two dashed lines in plate 5 can

be used for estimating riprap size. These criteria should not be used in lieu of model studies for large energy dissipators for reasons stated previously. The curve for small turbulent stilling basins should be used for minimum design type basins having lengths of 2.5 times or less the theoretically required tailwater depth d_2 and a design tailwater depth less than theoretical d_2. The curve for small stilling basins is considered applicable to basins with a length of $3d_2$ or greater and a design depth equal to theoretical d_2.

Bank Riprap

45. Whereas the bottom riprap stability problem is very complex, bank riprap below energy dissipators is more troublesome because of the combined effect of wave action and side rollers. Waves generated in a stilling basin contribute to the initial dislodgement of the rock and the side roller transports the material into the main current of flow below the stilling basin. There are numerous cases of severe bank erosion below stilling basins which has formed roughly semicircular indentations on each side of the outlet channels. The periodic replacement of bank riprap in these situations is, no doubt, a costly item.

Side rollers

46. The side rollers are more likely to be intense in the case of an abrupt termination of the vertical sidewalls of a stilling basin at an outlet channel of trapezoidal cross section. The suppression of side rollers by wing walls is described in the Engineer Manual on hydraulic design of reservoir outlet structures,[16] specifically paragraph 25i and plate 37 therein. It has been demonstrated in the laboratory that a wall with a circular quadrant extending to the channel side slope is effective in suppressing the side roller.

47. The appearance of the side roller on the surface is that of a simple eddy or vortex with a vertical axis of rotation. However, the toe of the side slope is normally in line with the base of the stilling basin wall so that the eddy axis must curve away from the bank and the diameter of the vortex decreases with increased depth. So far as is known, this

phenomenon with its special boundary geometry has not been fully explored experimentally. Regardless of the complexity of the problem, the hydraulic model study offers valuable assistance in designing to minimize the effect of the side roller upon the bank riprap below energy dissipators.

Wave action

48. Superimposed upon the side roller effect are substantial waves generated by the turbulence of a hydraulic jump or the impingement of a jet from a flip bucket. The following discussion is concerned principally with waves generated in a stilling basin. It can be expected that such waves from a jump with a high initial Froude number would be greater than those from a jump with a lower Froude number. Furthermore, waves in a jump foreshortened by baffles and an end sill should be larger than those from a simple jump on a flat floor.

49. The height of waves below a simple hydraulic jump on a flat floor was measured by Abou-Seida[17] at the University of California, Berkeley. The Berkeley tests were reanalyzed and plotted in plate 12 with entering Froude number F_1 versus H_s/d_1, where H_s is the observed wave height measured from crest to trough and d_1 is the depth of the flow entering the hydraulic jump. A relation was determined by least squares, eliminating the parameters where the sequent depth ratio d_2/d_1 was greater than 10 percent of the theoretical value. For reasons mentioned subsequently, the regression line was extrapolated from the upper limit of Abou-Seida's tests ($F_1 = 5.0$ to $F_1 = 10.0$).

50. The USBR measured wave heights in a model study of the stilling basin for Paonia Dam.[18] The plan and profile of this stilling basin are also shown in plate 12. It should be noted that the wave heights were measured near the water's edge. The maximum wave height observed is shown as a single point at $F_1 = 10$. The dashed line through this point is drawn parallel to the Abou-Seida regression line. Although such a line has little meaning because it involves a double extrapolation and a single stilling basin, no other guide is known for the problem of estimating wave heights in such a situation.

51. It can be concluded from the foregoing study that wave height observations in stilling basin model studies are very much needed. The

laboratory measurements can be accomplished with modern electronic apparatus. Preparations have been made by the WES in cooperation with the Fort Worth, Kansas City, and Louisville Districts to measure wave heights in the prototype when test flows are available. However, the laboratory offers a better opportunity to obtain information on a wider range of hydraulic and boundary geometry variables. If the designer has information on the approximate wave heights to be expected, the material on rock stability in the Engineer Manual on design of breakwaters and jetties[19] may be useful.

PART IV: CONCLUSIONS

52. Further information needed for riprap design is outlined in Appendix B. However, certain conclusions can be drawn from the study presented in this report, and are presented as follows.

a. The only known sound physical principle for stable rock design is the Airy law[7-9] which relates the weight of the stone to the sixth power of the mean velocity acting on the rock.

b. Only knowledge of the velocity profile near the bottom can be expected to yield a reasonable average velocity acting on the rock. The size of rock in turn affects the velocity distribution.

c. The mechanics of the stability of a given size rock within a wide span of size gradation needs more study. Further investigation may reveal that it is economical, where large quantities of riprap are to be placed, to screen out the smaller size rock for other uses, leaving a narrow span of size gradation.

d. The effect of flow in channel bends on riprap needs further study in the laboratory. In the meantime, the measurement of hydraulic variables in the field on both tangents and curves should yield early design information for a given size gradation.

e. The effectiveness of different designs of toe protection for riprap blankets needs to be investigated.

f. Riprap problems in connection with energy dissipators are so complex that they will require solution by the use of hydraulic models.

g. In general, the problem of the stability of riprap involves such an interrelation of independent and dependent variables that much more field and laboratory investigation is needed to permit development of the most economic design.

LITERATURE CITED

1. U. S. Army Engineer Waterways Experiment Station, CE, Hydraulic Design Criteria. Vols 1 and 2 (published serially by issues), Vicksburg, Miss.

2. Keulegan, G. H., "Law of turbulent flow in open channels." U. S. Bureau of Standards, Journal of Research, vol 21, No. 6, RP-1151 (Washington, D. C., December 1938), pp 707-741.

3. Engineering Hydraulics, Proceedings of the Fourth Conference, June 12-15, 1949, Hunter Rouse, ed. John Wiley & Sons, Inc., New York, N. Y., 1950, 1039 pp.

4. U. S. Army Engineer District, CE, Portland, Oregon, Report on High Velocity Revetment Tests (Civil Works Investigation 485). 1 January 1952.

5. U. S. Army Engineer Waterways Experiment Station, CE, Flow Characteristics in Flood-Control Tunnel 10, Fort Randall Dam, Hydraulic Prototype Tests. Technical Report No. 2-626, Vicksburg, Miss., June 1963.

6. Lundgren, H., and Jonsson, Ivan G., "Shear and velocity distribution in shallow channels." ASCE Hydraulics Division Journal, vol 90, HY 1 (January 1964), pp 1-21.

7. Shelford, William, "On rivers flowing into tideless seas, illustrated by the River Tiber." Proceedings, Institution of Civil Engineers, vol 82 (1885).

8. Airy, Wilfred, discussion of paper, "On rivers flowing into tideless seas, illustrated by the River Tiber," by William Shelford. Proceedings, Institution of Civil Engineers, vol 82 (1885), p 25.

9. Hooker, Elon H., "The suspension of solids in flowing water." Transactions, American Society of Civil Engineers, vol 36 (December 1896).

10. Isbash, S. V., "Construction of dams by depositing rock in running water." Transactions, Second Congress on Large Dams, vol 5 (1936), pp 123-136.

11. Lane, E. W., and Carlson, E. J., "Some factors affecting the stability of canals constructed in coarse granular materials." Proceedings, Minnesota International Hydraulics Convention (Minneapolis, Minn., September 1953), pp 37-48.

12. Ippen, A. T., and others, Stream Dynamics and Boundary Shear Distributions for Curved Trapezoidal Channels. Massachusetts Institute of Technology, Hydrodynamics Laboratory, Technical Report No. 47, Cambridge, Mass., January 1962.

13. U. S. Bureau of Reclamation, Boundary Shear Distribution Around a Curve in a Laboratory Canal. Progress Report No. 1, Hydraulics Branch Report No. Hyd-526, 26 June 1964.

14. Yen Ben-Chie, Characteristics of Subcritical Flow in a Meandering Channel. Institute of Hydraulic Research, University of Iowa, Iowa City, Iowa, 1965.

15. Preston, J. H., "The determination of turbulent skin friction by means of pitot tubes." Journal of the Royal Aeronautical Society, vol 58 (February 1954), pp 109-121.

16. U. S. Army, Office, Chief of Engineers, Hydraulic Design of Reservoir Outlet Structures. Engineer Manual 1110-2-1602, U. S. Government Printing Office, Washington, D. C., 1 August 1963.

17. Abou-Seida, M. M., "Wave action below spillways." ASCE Hydraulics Division Journal, vol 89, HY 3 (May 1963), pp 133-152.

18. U. S. Bureau of Reclamation, Hydraulic Model Studies of Paonia Dam Spillway and Outlet Works. Hydraulic Laboratory Report No. Hyd-444, Denver, Colo., 19 June 1959.

19. U. S. Army, Office, Chief of Engineers, Design of Breakwaters and Jetties. Engineer Manual 1110-2-2904, U. S. Government Printing Office, Washington, D. C., 30 April 1963.

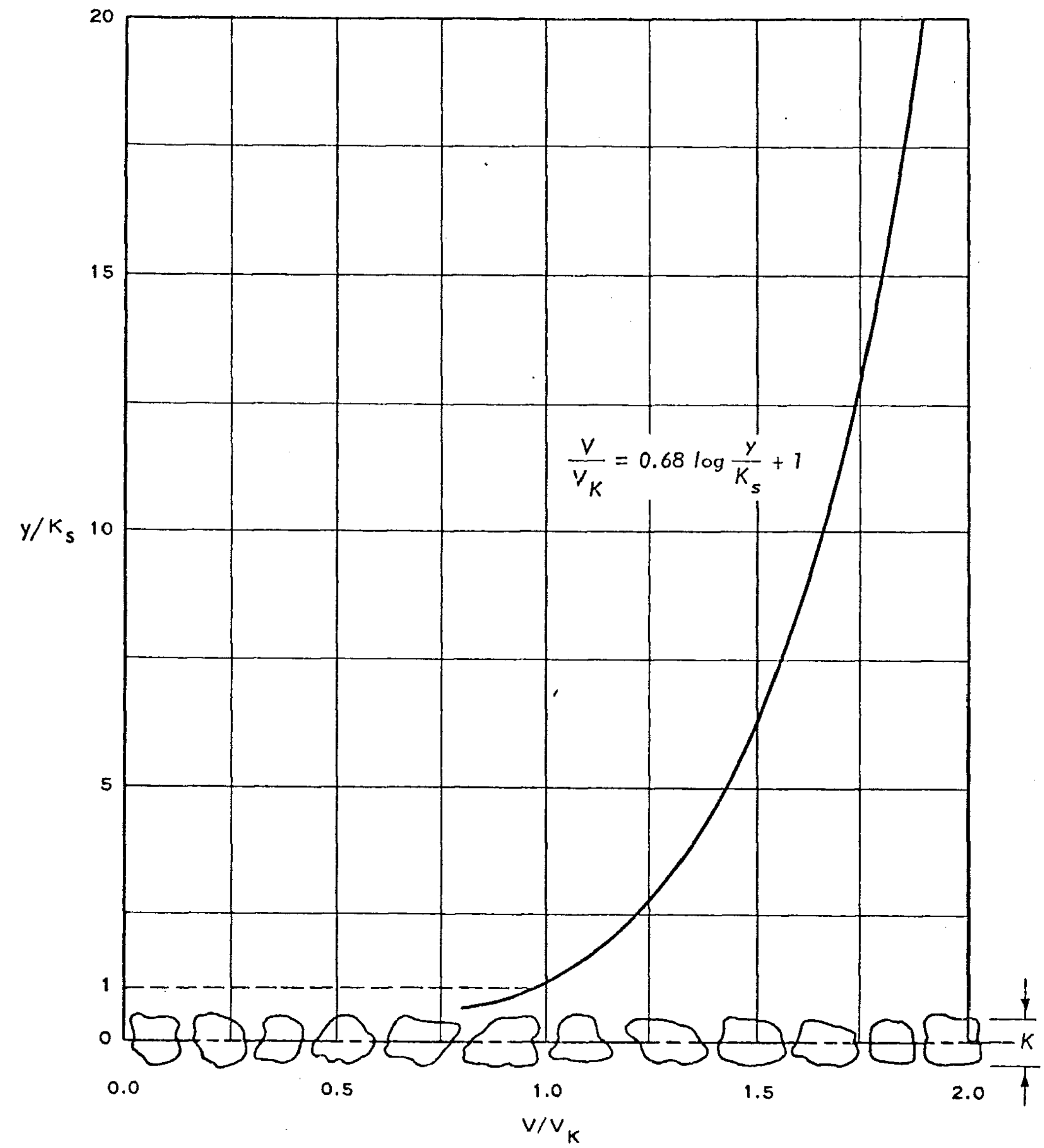

VELOCITY PROFILE
ROUGH BOUNDARY

PLATE 2

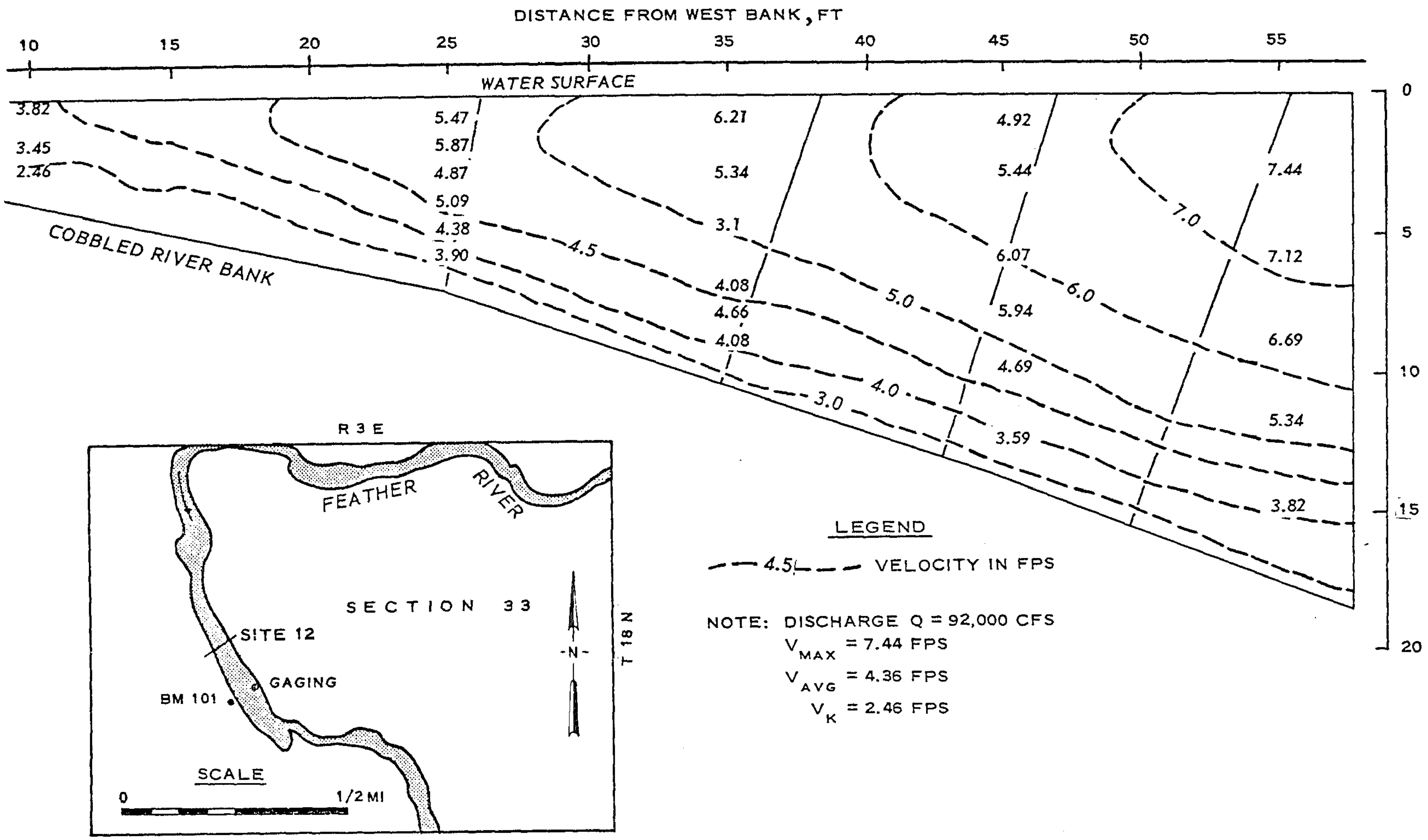

SITE LOCATION

VELOCITY DISTRIBUTION
FEATHER RIVER SITE 12

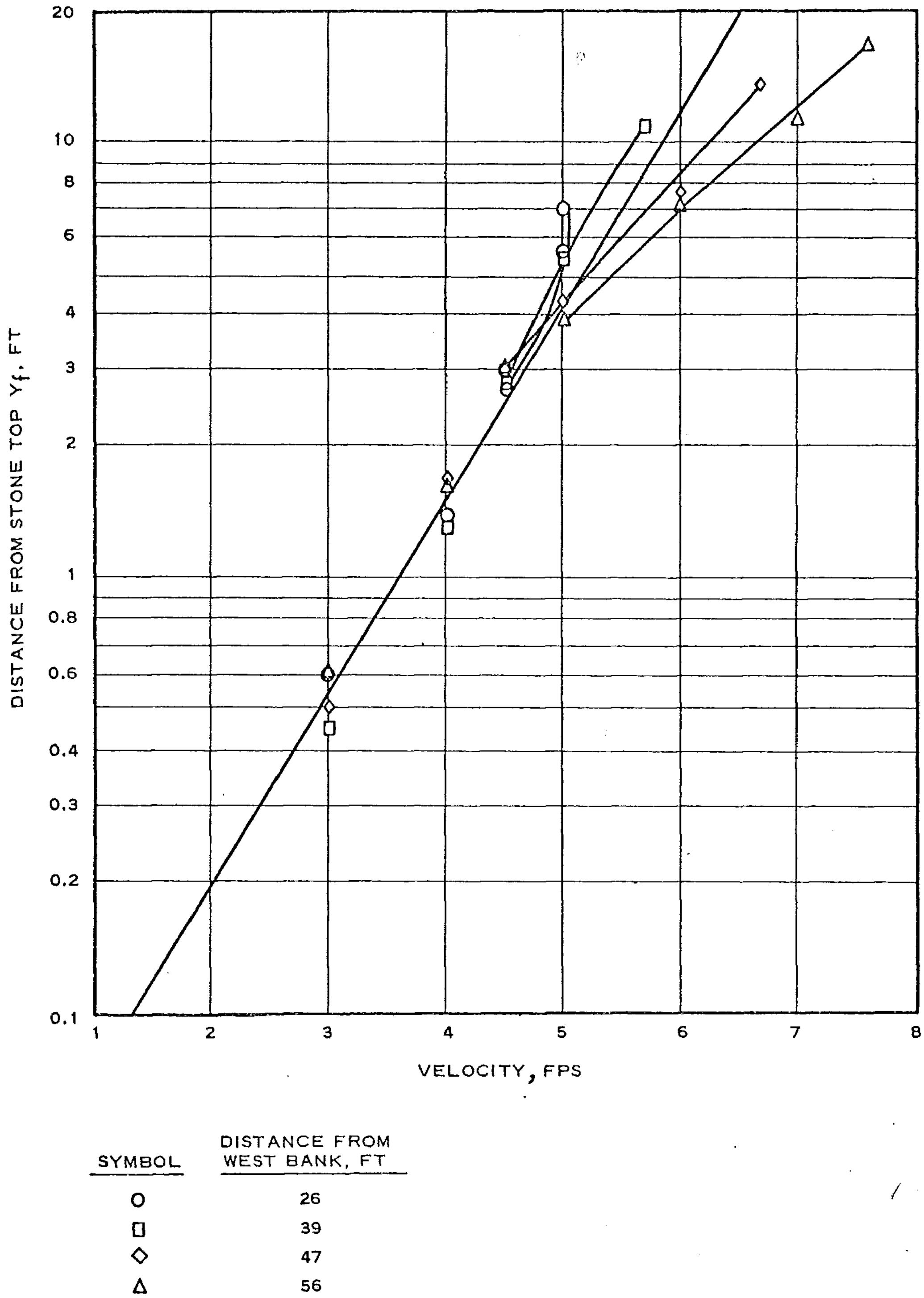

VELOCITY VERSUS Y_f
FEATHER RIVER SITE 12

PLATE 3

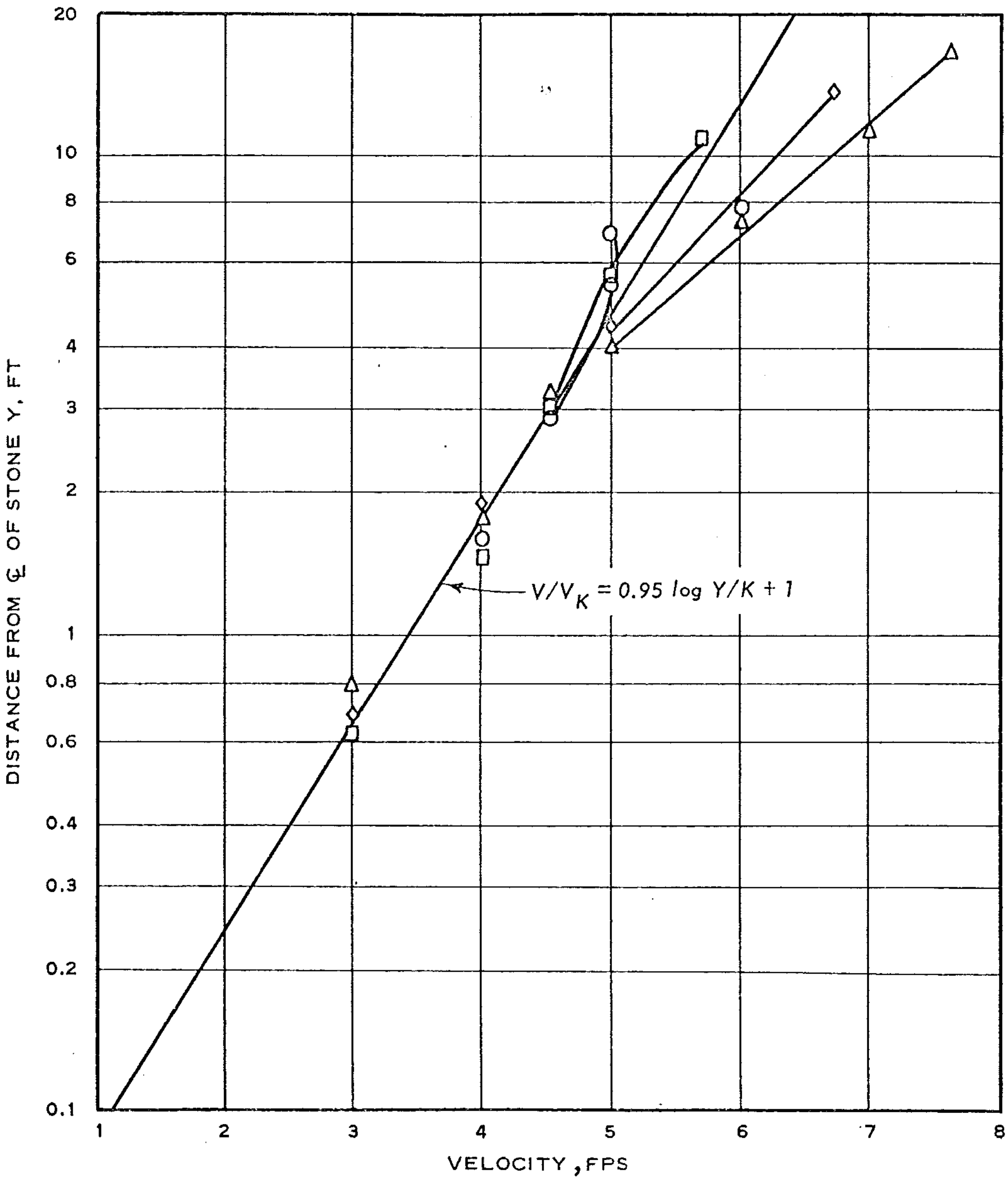

SYMBOL	DISTANCE FROM WEST BANK, FT
○	26
□	39
◇	47
△	56

K = 4.6 IN., 0.383'

V_K = 2.46 FPS

VELOCITY VERSUS Y
FEATHER RIVER SITE 12

PLATE 4

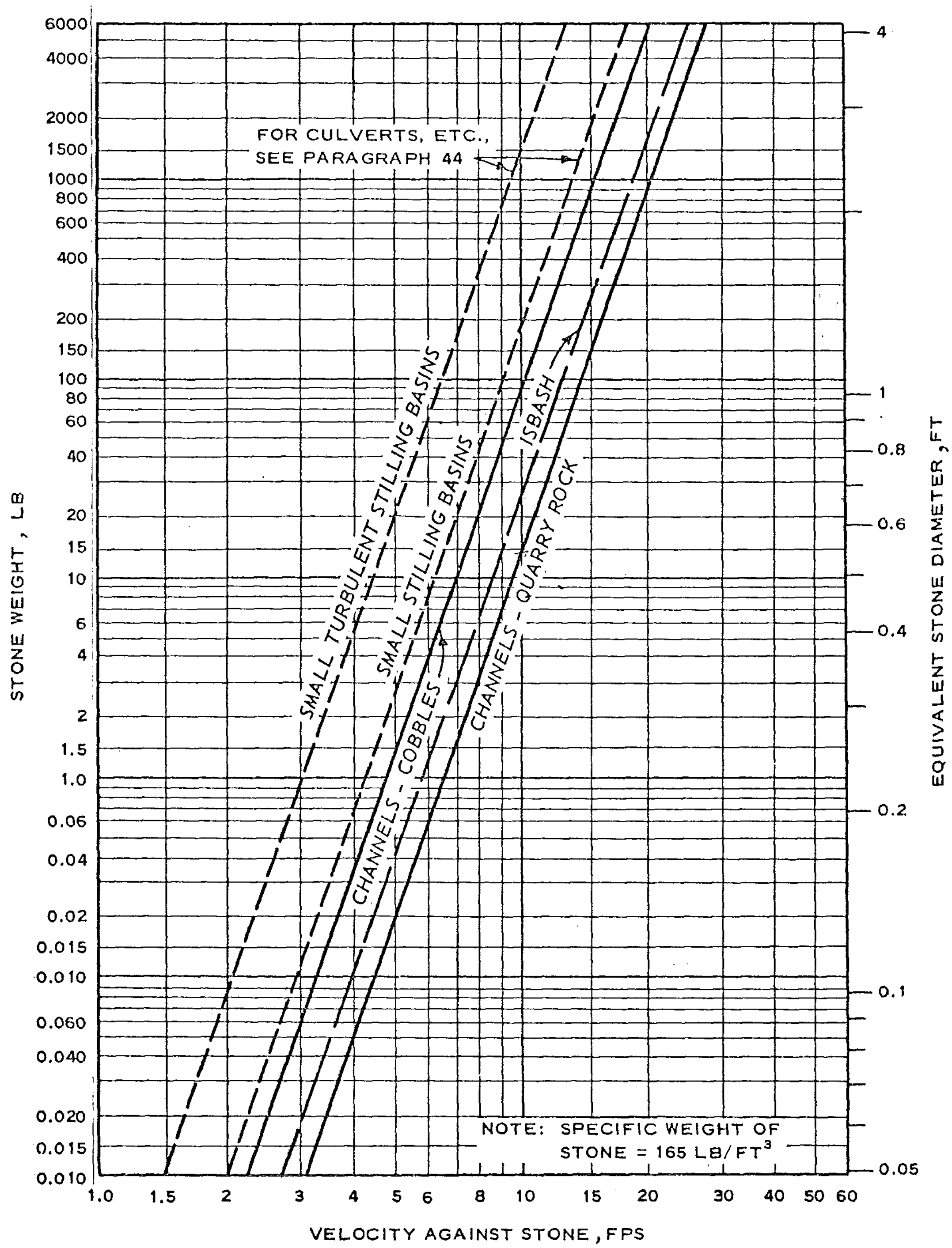

STABLE ROCK SIZE

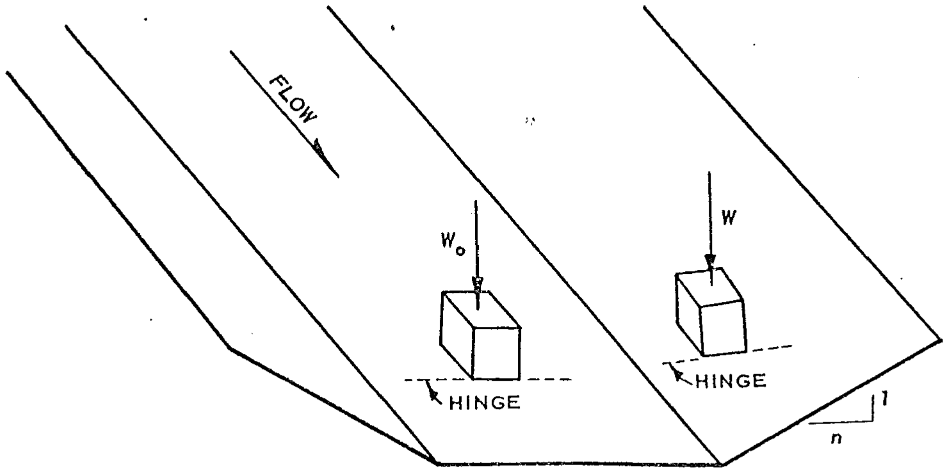

A. SCHEMATIC VIEW LOOKING UPSTREAM

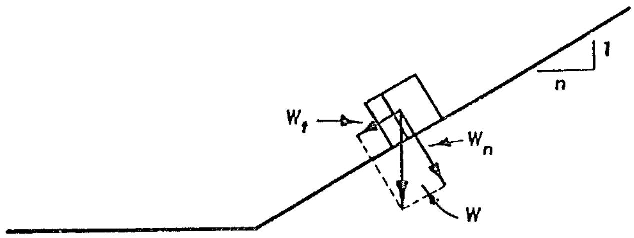

B. SECTION OF SLOPE WITH CUBE

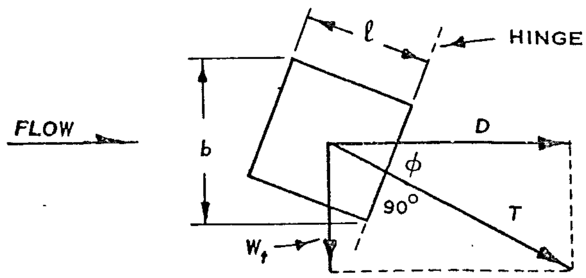

C. PLAN OF CUBE ON SLOPE

FORCES ACTING ON
BANK RIPRAP

PLATE 6

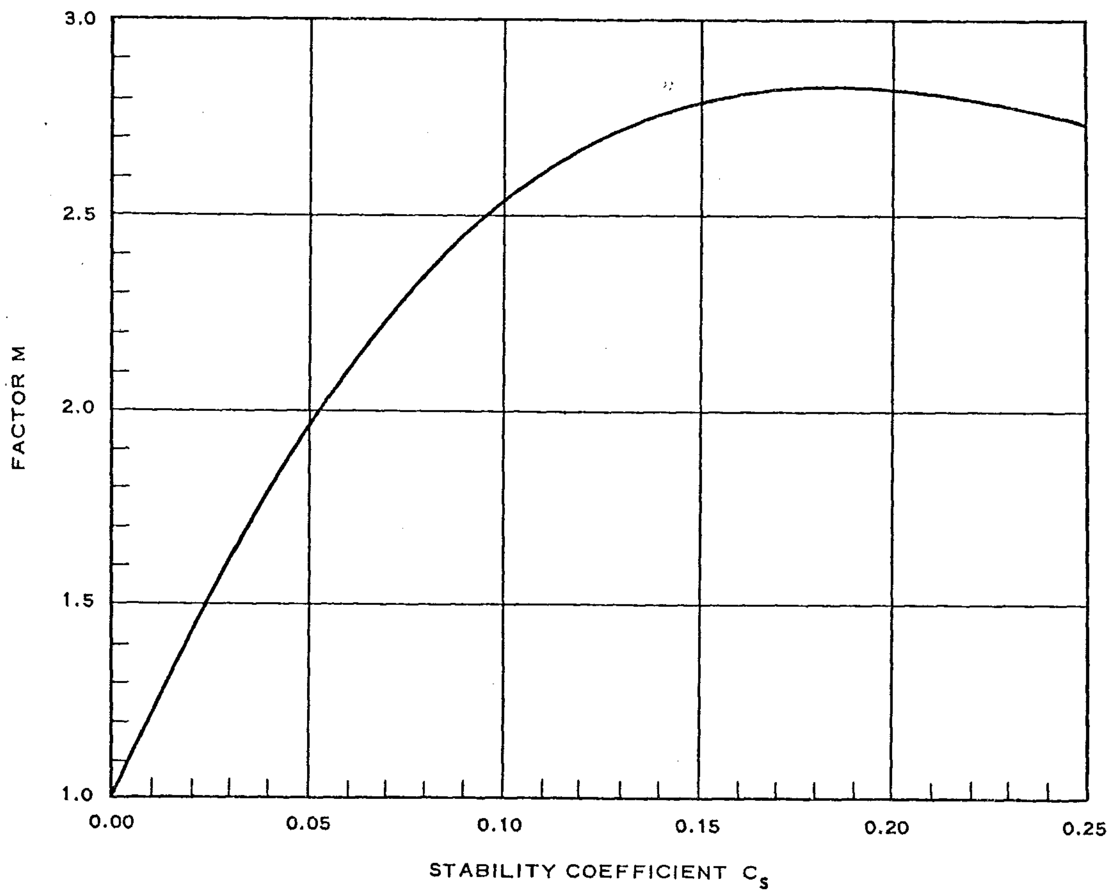

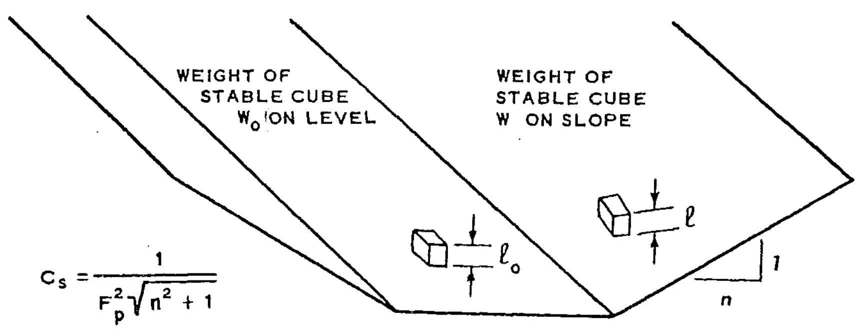

$$C_s = \frac{1}{F_p^2\sqrt{n^2 + 1}}$$

$$F_p = \frac{V_k}{\sqrt{g\ell}}$$

$$W = W_o M \left(\frac{n^2 + 1}{n^2 - 1}\right)^{3/2}$$

$$M = \left[1 + \sin(2\phi)\right]^{3/2}$$

NOTE: SEE PLATE 6 FOR DEFINITION OF ϕ.

STABILITY OF BANK RIPRAP

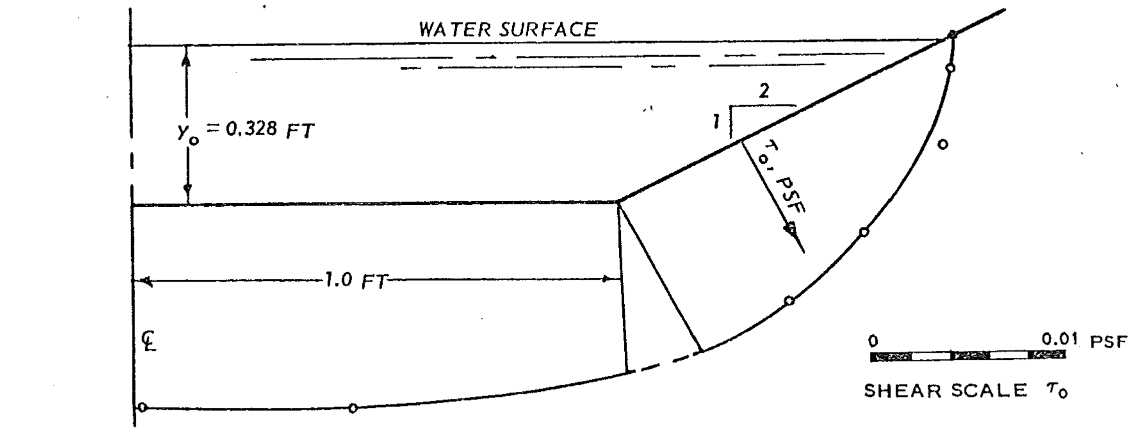

A. MIT ROUGH BOUNDARY TESTS

(STA 1, FIG. 20 IN REF 9 – STRAIGHT CHANNEL)

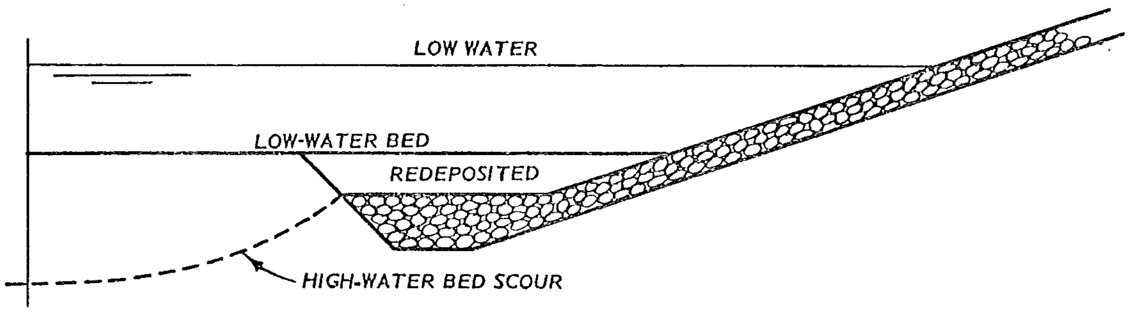

B. TOE TRENCH

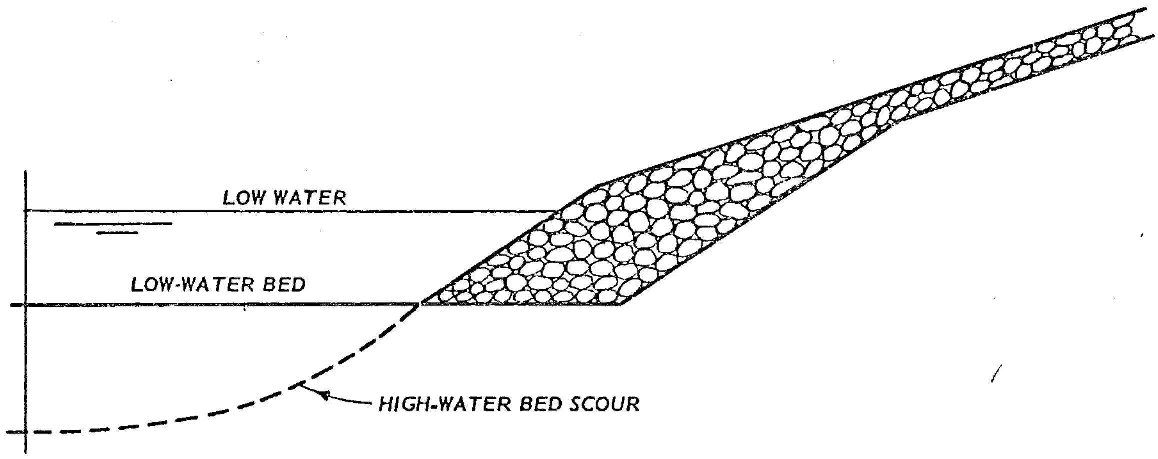

C. THICKENED TOE

RIPRAP TOE PROTECTION

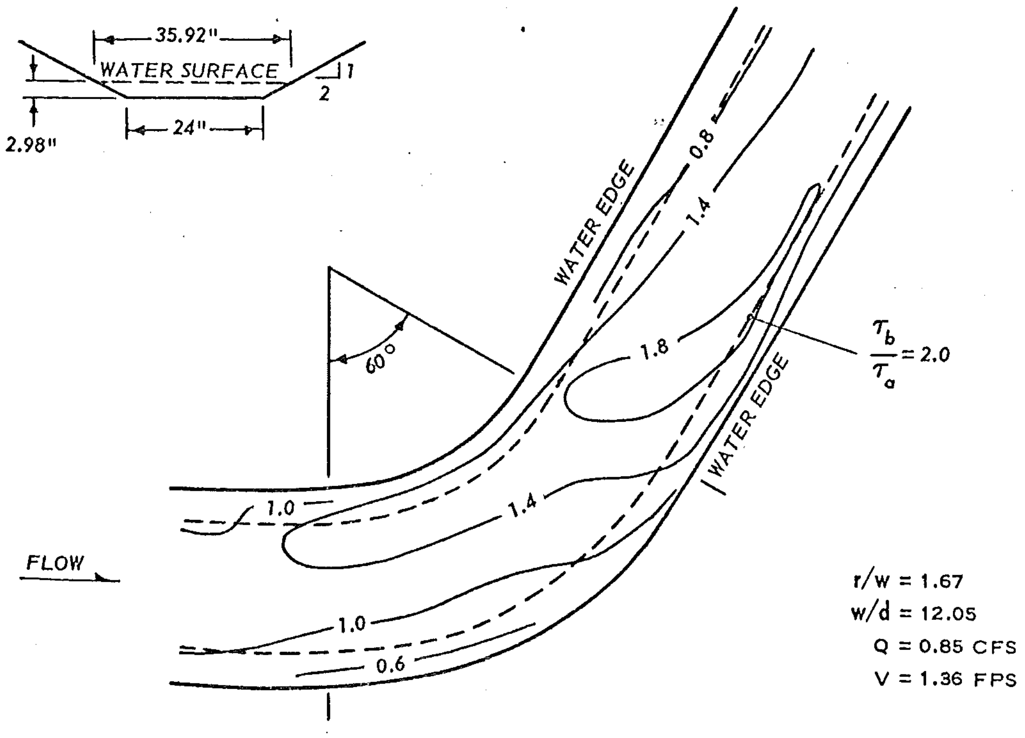

A. SMOOTH CHANNEL

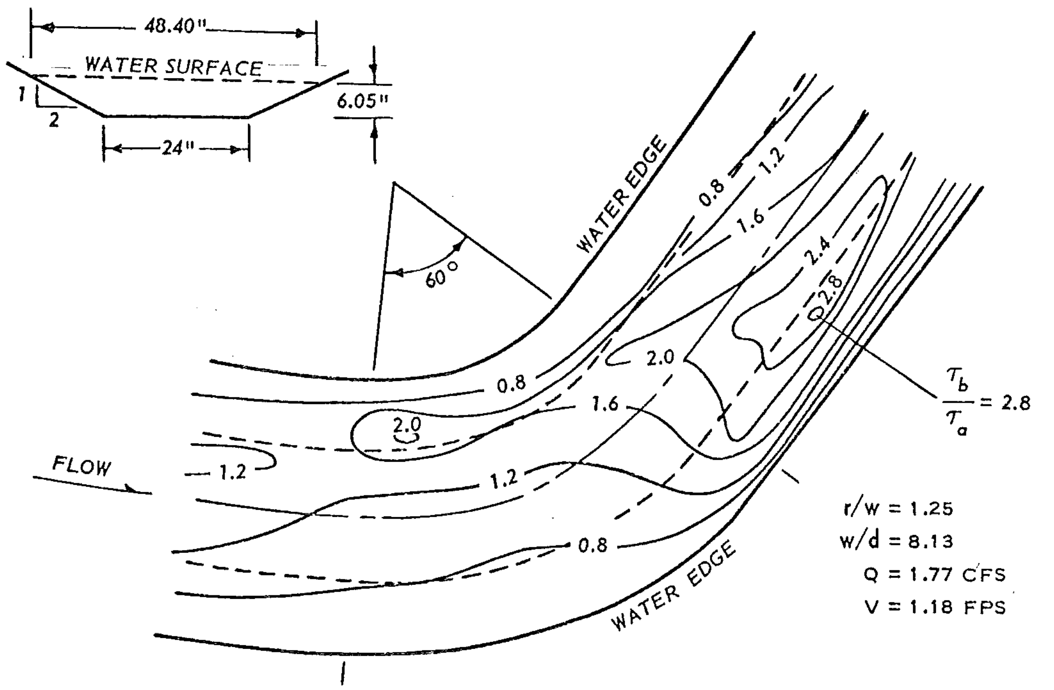

B. ROUGH CHANNEL

NOTE: FIGURES REPRODUCED FROM REF 12.

CHANNEL BEND EXPERIMENTS
MIT

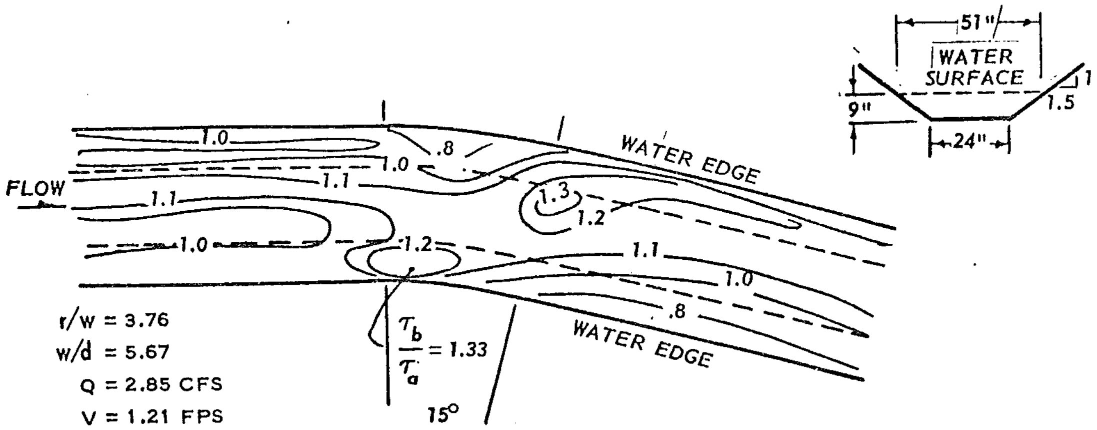

U. S. BUREAU OF RECLAMATION BEND
(SMOOTH CHANNEL, REF 13)

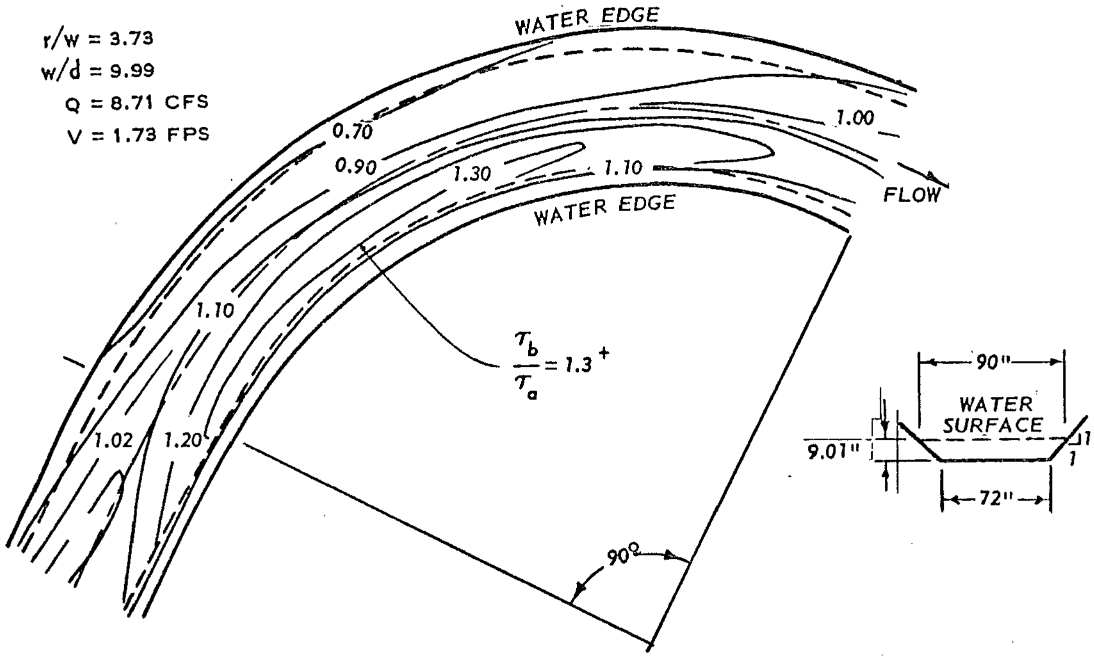

UNIVERSITY OF IOWA BEND
(SMOOTH CHANNEL, REF 14)

CHANNEL BEND EXPERIMENTS
USBR AND IOWA

PLATE 10

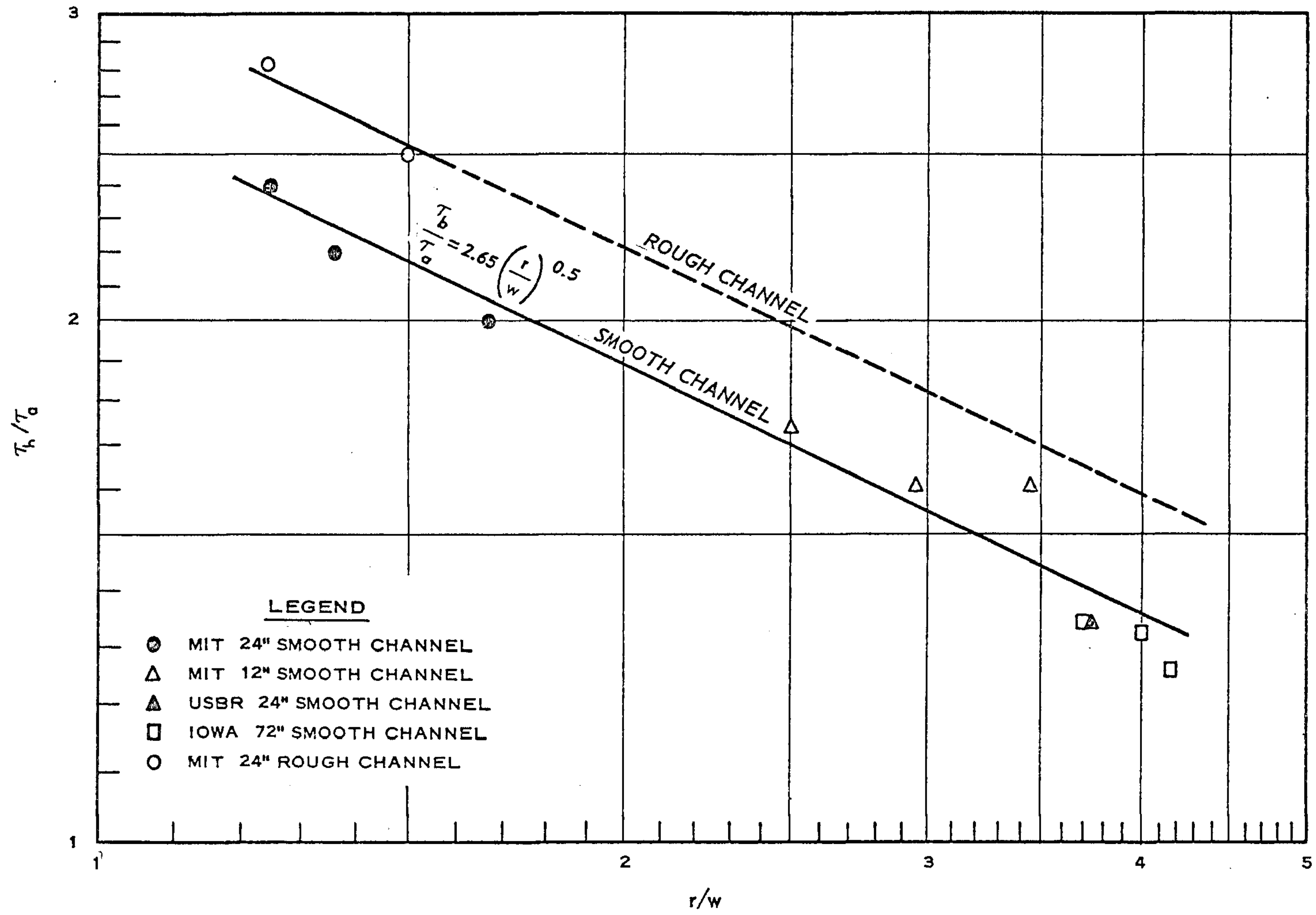

SHEAR IN CHANNEL BENDS

PLATE II

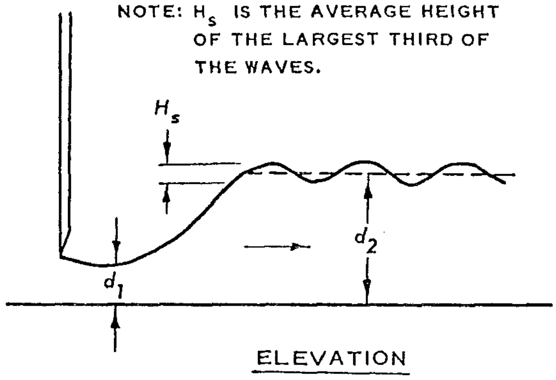

JUMP ON HORIZONTAL BED
(REF 17)

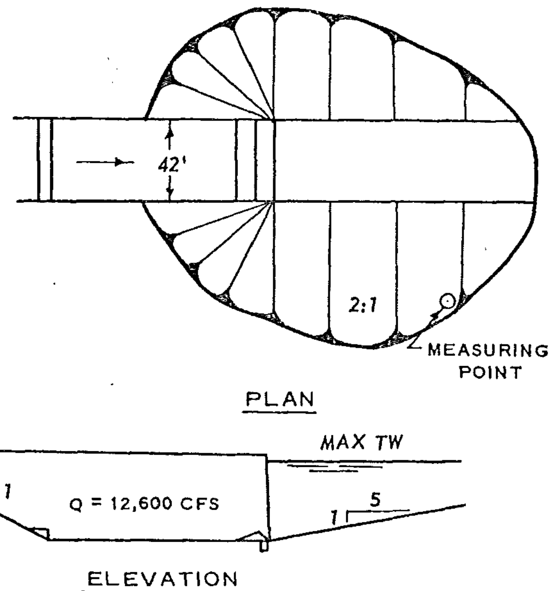

PAONIA STILLING BASIN
(REF 18)

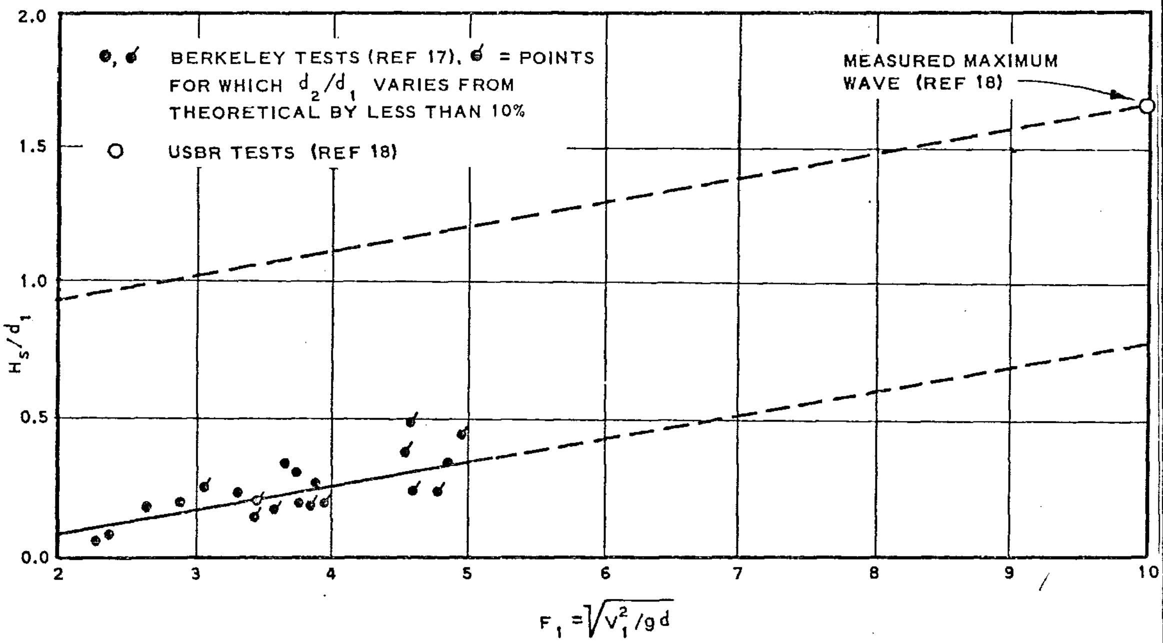

WAVES BELOW HYDRAULIC JUMPS

PLATE 12

APPENDIX A: STABILITY OF CUBICAL RIPRAP ELEMENTS OF BANK SLOPES

1. This appendix discusses the stability of a cubical element on the side slopes of a channel. The cube is subjected to two forces, its weight W and a fluid drag force D proportional to the frontal area of the element. It is assumed that the overturning force T acts at right angles to a face of the cube and that the cube fails by overturning. A definition of these and other forces is given in plate 6 of the main text.

2. The weight can be resolved into two components W_n and W_t, such that W_n acts normal to the sloping bank and W_t acts tangent to the bank.

$$W_n = \frac{n}{\sqrt{n^2 + 1}} W \qquad \text{(A1)}$$

$$W_t = \frac{1}{\sqrt{n^2 + 1}} W \qquad \text{(A2)}$$

But the weight itself can be written as

$$W = (\gamma_p - \gamma_f)\, \ell^3 \qquad \text{(A3)}$$

where γ_p and γ_f are the specific weights of the particle and the fluid, respectively. Setting $\gamma_p - \gamma_f = \gamma_s$, the submerged specific weight of the particle,

$$W = \gamma_s \ell^3 \qquad \text{(A4)}$$

The drag force D is given by

$$D = C_d A_f \gamma_f \frac{V_K^2}{2g} \qquad \text{(A5)}$$

where A_f is the frontal area, V_K is the velocity at a height $\ell/2$ above the top of the cube, and C_D is a drag coefficient.

Since

$$A_f = b\ell = \ell^2 (\sin \phi + \cos \phi) \qquad \text{(A6)}$$

hence

$$D = C_d \ell^2 (\sin \phi + \cos \phi) \gamma_f \frac{V_K^2}{2g} \tag{A7}$$

Because T acts at right angles to the hinge,

$$\tan \phi = \frac{W_T}{D} = \frac{\gamma_s \ell^3 / \sqrt{n^2 + 1}}{C_D \ell^2 \gamma_f \frac{V_K^2}{2g} (\sin \phi + \cos \phi)} \tag{A8}$$

and

$$\tan \phi (\sin \phi + \cos \phi) = \frac{2\gamma_s}{\sqrt{n^2 + 1}\, C_D \gamma_f} \times \frac{g\ell}{V_K^2} \tag{A9}$$

Defining F_p , a particle Froude number, as

$$F_p = \frac{V_K}{\sqrt{g\ell}} \tag{A10}$$

equation A9 becomes

$$\tan \phi (\sin \phi + \cos \phi) = \frac{2\gamma_s}{\sqrt{n^2 + 1}\, C_D \gamma_f F_p^2} \tag{A11}$$

The overturning force T is

$$T = \sqrt{D^2 + W_t^2}$$

$$= \sqrt{C_D^2 \ell^4 (1 + 2 \sin \phi \cos \phi) \gamma_f^2 \frac{V_K^4}{4g^2} + \frac{\gamma_s^2 \ell^6}{n^2 + 1}} \tag{A12}$$

Summing the moments about the hinge edge and assuming that the forces pass through the center of gravity of the cube result in:

$$\left(\frac{\ell}{2}\right) T = \left(\frac{\ell}{2}\right) W_n$$

or

$$T = W_n \tag{A13}$$

The squares of T and W_n are equated to obtain

$$C_D^2 \ell^4 (1 + 2 \sin \phi \cos \phi) \gamma_f^2 \frac{V_K^4}{4g^2} + \frac{\gamma_s^2 \ell^6}{n^2 + 1} = \frac{n^2 \gamma_s^2 \ell^6}{n^2 + 1}$$

$$C_D^2 (1 + 2 \sin \phi \cos \phi) \gamma_f^2 \frac{V_K^4}{4g^2} + \frac{\gamma_s^2 \ell^2}{n^2 + 1} = \frac{n^2 \gamma_s^2 \ell^2}{n^2 + 1} \qquad \text{(A14)}$$

Solving for ℓ^2 results in

$$\ell^2 = \frac{C_D^2 (1 + 2 \sin \phi \cos \phi) \gamma_f^2 \frac{V_K^4}{4g^2}}{\frac{n^2 \gamma_s^2 - \gamma_s^2}{n^2 + 1}}$$

$$= \frac{n^2 + 1}{n^2 - 1} \left(\frac{\gamma_f}{\gamma_s}\right)^2 (1 + 2 \sin \phi \cos \phi) \frac{V_K^4}{4g^2} C_D^2 \qquad \text{(A15)}$$

On a level bed $n \to \infty$ and $\phi = 0$

$$\ell_o = \frac{C_D V_K^2 \gamma_f}{2 \gamma_s g} \qquad \text{(A16)}$$

Nondimensionalizing ℓ by ℓ_o

$$\frac{\ell}{\ell_o} = \left[\frac{n^2 + 1}{n^2 - 1} (1 + 2 \sin \phi \cos \phi)\right]^{1/2}$$

$$= \left\{\frac{n^2 + 1}{n^2 - 1} [1 + \sin (2\phi)]\right\}^{1/2} \qquad \text{(A17)}$$

Since the weight of a particle is proportional to its length cubed

$$\frac{W}{W_o} = \left\{\frac{n^2 + 1}{n^2 - 1} [1 + \sin (2\phi)]\right\}^{3/2} \qquad \text{(A18)}$$

Plate 5 gives

$$W_{od} = 1.22 \times 10^{-5} V_K^6 \qquad \text{(A19)}$$

for quarry rock, W_{od} being the dry weight of the stone. Since

$$W_{od} = \gamma_p \frac{C_D^3 V_K^6 \gamma_f^3}{8\gamma_s^3 g^3} \qquad (A20)$$

then

$$C_D = \left[\frac{(1.22 \times 10^{-5})(8g^3)(\gamma_s^3)}{\gamma_p \gamma_f^3}\right]^{1/3} \qquad (A21)$$

If $\gamma_p = 165\ lb/ft^3$ and $\gamma_f = 62.4\ lb/ft^3$,

$$C_d = 0.444 \qquad (A22)$$

The angle ϕ can now be found using equation All. Using $\gamma_p = 165\ lb/ft^3$ and $C_D = 0.444$

$$\tan \phi\ (\sin \phi + \cos \phi) = 7.41\ (n^2 + 1)^{-1/2}\ F_p^{-2} \qquad (A23)$$

Since this is a rather difficult expression to work with, a table of $(1/7.41) \tan \phi\ (\sin \phi + \cos \phi)$ has been prepared and graphed against $[1 + \sin (2\phi)]^{3/2}$. In the following tabulation

$$C_s = (n^2 + 1)^{-1/2}\ F_p^{-2} = \frac{\tan \phi\ (\sin \phi + \cos \phi)}{7.41} \qquad (A24)$$

$$M = [1 + \sin (2\phi)]^{3/2} \qquad (A25)$$

ϕ, deg	C_s	M
0	0.0000	1.000
10	0.0276	1.555
20	0.0631	2.105
30	0.1057	2.550
40	0.1595	2.800
50	0.2270	2.800
60	0.3194	2.550
70	0.4760	2.105
80	0.8850	1.555
90	∞	1.000

Equation A18 becomes

$$\frac{W}{W_o} = \left(\frac{n^2 + 1}{n^2 - 1}\right) M \qquad \text{(A26)}$$

M is given as a function of C_s in plate A1 for 0 deg $\leq \phi \leq$ 80 deg, and in plate 7 of the main text for 0 deg $\leq \phi \leq$ 55 deg.

3. Sample computations illustrating two procedures for determining the cube size required for stability on side slopes are presented below. In the first example, the principle of successive approximation is used. The principle of trial and error is used in the second illustration.

EXAMPLE 1

Given:

W_o = 97 lb, V_K = 14.4 fps
Specific weight of rock = 165 lb/ft^3
Bank slope = 1/n; n = 6

Computation:

1. Assume $W = W_o$ (1st approximation) and estimate Froude number of particle on slope

$$\gamma \ell^3 = 97 \qquad \text{(A4)}$$

$$\ell = 0.838 \text{ ft}$$

$$F_p = V_K/\sqrt{g\ell} = 14.4/\sqrt{32.2\ (0.838)} \qquad \text{(A10)}$$

$$= 2.77$$

2. Calculate C_s for F_p = 2.77

$$C_s = \frac{1}{F_p^2\sqrt{n^2 + 1}} \qquad \text{(A24)}$$

$$C_s = \frac{1}{(2.77)^2\ (6.08)} = 0.214$$

3. From plate 7 obtain

$$M = 1.43 \text{ for } C_s = 0.021$$

4. Calculate W (2d approximation)

$$W = W_o M \left(\frac{n^2 + 1}{n^2 - 1} \right)^{3/2} \qquad \text{(A18 and A25)}$$

$$= (97)(1.43)(1.09) = 151 \text{ lb}$$

5. Check F_p

$$W = 151 \text{ lb}$$

$$\gamma \ell^3 = 151$$

$$\ell = 0.971 \text{ ft}$$

$$F_p = 14.4/\sqrt{32.2\ (0.971)}$$

$$= 2.58$$

Since the Froude numbers calculated in steps 1 and 5 are substantially different, steps 2-5 should be repeated.

2a. Calculate C_s for $F_p = 2.58$

$$C_s = \frac{1}{(2.58)^2\ (6.08)} = 0.0249$$

3a. From plate 7 obtain

$$M = 1.53 \text{ for } C_s = 0.025$$

4a. Calculate W (3d approximation)

$$W = (97)(1.53)(1.09) = 162 \text{ lb}$$

5a. Check F_p

$$W = 162 \text{ lb}$$

$$\gamma \ell^3 = 162$$

$$\ell = 0.994$$

$$F_p = 14.4/\sqrt{32.2\ (0.994)}$$

$$= 2.55$$

Since the Froude numbers calculated in steps 5 and 5a agree reasonably well, the process is complete and W = 162 lb.

EXAMPLE 2

The successive approximation process used in example 1 can be virtually eliminated by arbitrarily increasing the M value found in step 3 as illustrated below.

Given:

W_o = 97 lb, V_K = 14.4 fps

Specific weight of rock = 165 lb/ft^3

Bank slope = 1/n; n = 2

Computation:

1. Assume $W = W_o$ (1st approximation) and estimate Froude number of particle on slope

$$\gamma \ell^3 = 97 \text{ lb} \qquad \text{(A4)}$$

$$\ell = 0.838 \text{ ft}$$

$$F_p = V_K/\sqrt{g\ell} = 14.4/\sqrt{32.2\ (0.838)} \qquad \text{(A10)}$$

$$= 2.81$$

2. Calculate C_s for F_p = 2.81

$$C_s = \frac{1}{F_p^2\sqrt{n^2 + 1}} \qquad \text{(A24)}$$

$$C_s = \frac{1}{(2.81)^2\ (2.24)} = 0.0565$$

3. From plate 7 obtain

$$M = 2.05 \text{ for } C_s = 0.057$$

As explained above, M should be arbitrarily increased; use $M = 2.5$

4. Calculate W (2d approximation)

$$W = W_o M \left(\frac{n^2 + 1}{n^2 - 1}\right)^{3/2} \qquad \text{(A18 and A25)}$$

$$= (97)(2.5)(2.15) = 522 \text{ lb}$$

5. Check the M assumed in step 3

a. Compute cube size

$$\gamma \ell^3 = 522 \text{ lb}$$

$$\ell = 1.47 \text{ ft}$$

b. Compute Froude number F_p

$$F_p = 14.4/\sqrt{32.2\ (1.47)}$$

c. Compute C_s

$$C_s = \frac{1}{(2.09)^2\ (2.24)} = 0.102$$

d. From plate 7 obtain

$$M = 2.53 \text{ for } C_s = 0.102$$

Since the M assumed in step 3 agrees reasonably well with that of step 5, the process is complete and $W = 522$ lb.

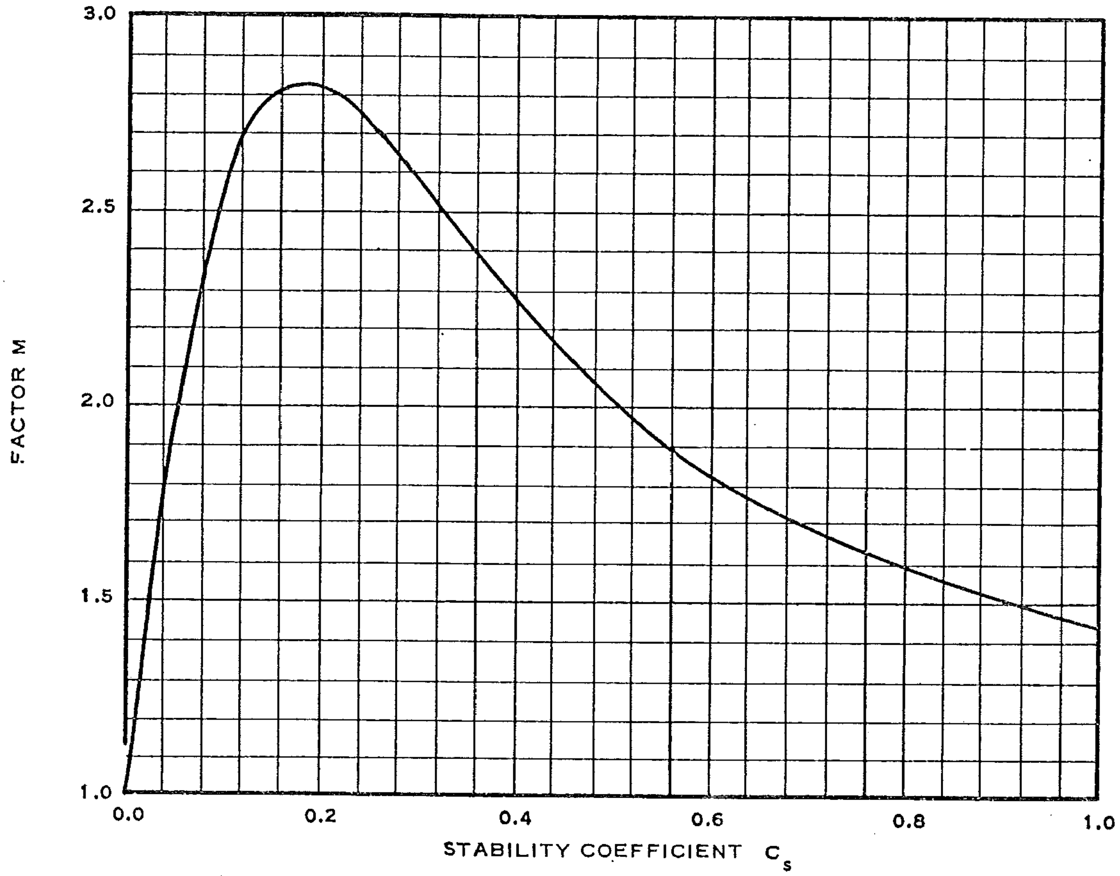

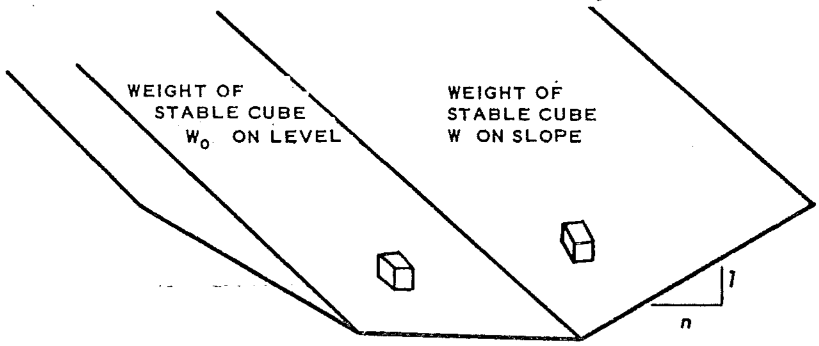

$$C_s = \frac{1}{F_p^2\sqrt{n^2+1}}$$

$$F_p = \frac{V_K}{\sqrt{g\ell}}$$

$$W = W_o M \left(\frac{n^2+1}{n^2-1}\right)^{3/2}$$

$$M = [1 + SIN\ (2\phi)]^{3/2}$$

NOTE: SEE PLATE 6 FOR DEFINITION OF ϕ.

CUBE STABILITY ON SLOPES

PLATE AI

APPENDIX B: RIPRAP INVESTIGATIONS NEEDED

Field Observations

Straight channels

1. Character of riprap placed
   - a. Method of placement and thickness
   - b. Size gradation
   - c. Shape characteristics (photographs of typical stones)
2. Stream measurements (both bank and bottom)
   - a. Vertical velocity measurements
   - b. Full cross section showing depths
   - c. Character of bed and scour estimate
   - d. Longitudinal water-surface profile for slope
3. Analysis of velocity profiles
   - a. Composite velocity profiles from isovels
   - b. Estimate of effective roughness size K
   - c. Estimate of effective velocity V_K
   - d. Estimate of stable size rock (bottom and bank)
4. Study of design flood stage
   - a. Effect of increased depth
   - b. Effect of water-surface slope change
   - c. Estimated design velocity V_K
5. Study of rock dislodgement
   - a. Marking of typical size rock and record of location
   - b. Observation of dislodged rock after flood
   - c. Comparison of stable size with estimated size

Channel bends

Repeat field measurements as indicated for straight channels, and also obtain the following.

1. Bend characteristics
   - a. Map for width and radius estimate
   - b. Cross sections for thalweg location and general bed shape

2. Analysis of field observations

   a. Comparison of V_K with that for straight channels

   b. Comparison of V_K with laboratory tests

   c. Comparison of stable rock size with that for straight channel

3. Toe protection (toe trench or thickened toe)

   a. Record of placement

   b. Estimate of scour

   c. Postflood examination of effectiveness

Laboratory Investigations

Flume studies (uniform flow)

1. Effect of bottom roughness on velocity profile

   a. Uniform size roughness elements

   b. Gradation of size of elements

2. Effect of bottom velocity on stone movement

   a. Single size

   b. Graded sizes

3. Bends of triangular cross section

Stilling basin models

1. Measured size gradation
2. Vertical velocity profiles in problem areas
3. Observations of stone dislodgement for specific bottom velocities
4. Measurement of wave heights below stilling basins
5. Three-dimensional observation of velocity distribution in a side roller